https://doi.org/10.1093/plcell/koac026 THE PLANT CELL 2022: 34: 2001–2018

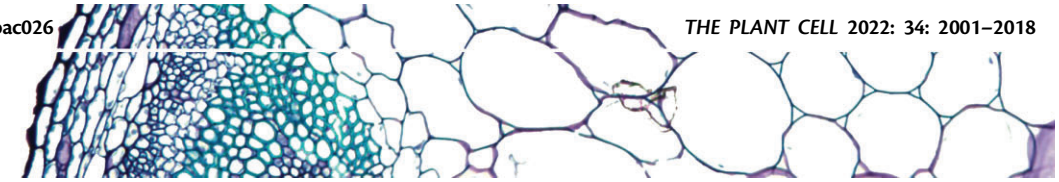

Research Article

The tomato OST1–VOZ1 module regulates drought-mediated flowering

Leelyn Chong [1,2], Rui Xu [1,2], Pengcheng Huang [1,2], Pengcheng Guo [1,2], Mingku Zhu [3], Hai Du [4], Xiaoli Sun [5], Lixia Ku[6], Jian-Kang Zhu [7,8] and Yingfang Zhu [1,2,*,†]

1 State Key Laboratory of Crop Stress Adaptation and Improvement, School of Life Sciences, Henan University, Kaifeng 475001, China
2 Sanya Institute of Henan University, Sanya, 572025, China
3 Institute of Integrative Plant Biology, School of Life Sciences, Jiangsu Normal University, Xuzhou 221116, China
4 College of Agronomy and Biotechnology, Chongqing Engineering Research Center for Rapeseed, Southwest University, Chongqing 400716, China
5 Crop Stress Molecular Biology Laboratory, Heilongjiang Bayi Agricultural University, Daqing 163319, China
6 College of Agronomy, Synergetic Innovation Center of Henan Grain Crops and National Key Laboratory of Wheat and Maize Crop Science, Henan Agricultural University, Zhengzhou 450046, China
7 Shanghai Center for Plant Stress Biology, Shanghai Institutes for Biological Sciences, Chinese Academy of Sciences, Shanghai 200032, China
8 Department of Horticulture and Landscape Architecture, Purdue University, West Lafayette, Indiana 47907, USA

*Author for correspondence: zhuyf@henu.edu.cn
These authors contributed equally (L.C., R.X., and P.H.).
†Senior author

Y.Z. designed the study. L.C., R.X., P.H., P.G., M.Z., H.D., and X.S. performed the experiments. J.K.Z., L.K., and Y.F.Z. analyzed the data. L.C. and Y.Z. wrote the manuscript. The authors declared no conflicts of interest.
The author responsible for distribution of materials integral to the findings presented in this article in accordance with the policy described in the Instructions for Authors (https://academic.oup.com/plcell) is: Yingfang Zhu (zhuyf@henu.edu.cn).

Abstract

Flowering is a critical agricultural trait that substantially affects tomato fruit yield. Although drought stress influences flowering time, the molecular mechanism underlying drought-regulated flowering in tomato remains elusive. In this study, we demonstrated that loss of function of tomato OPEN STOMATA 1 (SlOST1), a protein kinase essential for abscisic acid (ABA) signaling and abiotic stress responses, lowers the tolerance of tomato plants to drought stress. *slost1* mutants also exhibited a late flowering phenotype under both normal and drought stress conditions. We also established that SlOST1 directly interacts with and phosphorylates the NAC (NAM, ATAF and CUC)-type transcription factor VASCULAR PLANT ONE-ZINC FINGER 1 (SlVOZ1), at residue serine 67, thereby enhancing its stability and nuclear translocation in an ABA-dependent manner. Moreover, we uncovered several SlVOZ1 binding motifs from DNA affinity purification sequencing analyses and revealed that SlVOZ1 can directly bind to the promoter of the major flowering-integrator gene *SINGLE FLOWER TRUSS* to promote tomato flowering transition in response to drought. Collectively, our data uncover the essential role of the SlOST1–SlVOZ1 module in regulating flowering in response to drought stress in tomato and offer insights into a novel strategy to balance drought stress response and flowering.

Received September 20, 2021. Accepted January 25, 2022. Advance access publication January 31, 2022

IN A NUTSHELL

Background: Flowering in tomato (*Solanum lycopersicum*) is a crucial developmental stage that can be hindered by environmental stresses such as drought. Prolonged exposure to drought at this stage can result in significant yield losses because drought stress threatens the growth and development of plants. Flowering has been reported as one of the mechanisms that plants utilize to respond to drought and hasten the production of seeds to ensure species survival.

Question: How does tomato know how to balance drought responses and flowering time? We investigated this question by examining the tomato ortholog to the kinase Open Stomata 1 (SlOST1), as OST1 is critical for abscisic acid (ABA) signaling, abiotic stress responses and regulation of stomatal movement in Arabidopsis and several other plant species, raising the possibility that OST1 may play a role in flowering.

Findings: We found that tomato SlOST1 not only positively regulates drought tolerance but also promotes flowering under drought stress conditions. We also discovered that SlOST1 promotes the stability and nuclear translocation of the NAC-type transcription factor VASCULAR PLANT ONE-ZINC FINGER 1 (SlVOZ1) via phosphorylation, which is further enhanced by ABA. In addition, we revealed that nucleus-localized SlVOZ1 can bind to the promoter of a major flowering gene *SINGLE FLOWER TRUSS (SFT)* to modulate flowering. It was intriguing to discover the essential role of the SlOST1-SlVOZ1 module in balancing flowering and drought stress response in tomato.

Next steps: From previous and current studies, it is clear that OST1 is involved in various biological functions. The *slost1* mutant plants of our study were smaller than the wild type, so we will be investigating the role of SlOST1 in tomato growth and development regulation next.

Introduction

Drought is a major abiotic stress that dramatically limits plant growth and crop productivity. Drought stress triggers the biosynthesis of abscisic acid (ABA), which is essential in helping plants adapt and activate drought stress responses (Zhu, 2016; Chen et al., 2020a, 2020b). The ABA signaling pathway involves three core components: the receptors PYRABACTIN RESISTANT (PYR)/PYR1-like /REGULATORY COMPONENT OF ABA RESPONSES; negative regulators belonging to the Clade A protein phosphatase 2C family; and protein kinases from the sucrose nonfermenting 1-related protein kinase 2 family (SnRK2), whose downstream substrates include key transcription factors (TFs) and ion channels (Nakashima and Yamaguchi-Shinozaki, 2013; Hou et al., 2016; Chong et al., 2020; Zhu et al., 2020). SnRK2s elicit stress responses by regulating the interplay between different signaling pathways (Coello et al., 2011; Kulik et al., 2011; Fujii and Zhu, 2012). In particular, SnRK2.2, SnRK2.3, and SnRK2.6 (also named OPEN STOMATA 1 [OST1]) are activated by ABA and positively regulate ABA signaling and abiotic stress responses (Mustilli et al., 2002; Fujii et al., 2007; Nakashima et al., 2009; Fujita et al., 2009; Zhu, 2016). SnRK2.6/OST1/SRK2E has been studied most extensively for its role in responses to various environmental stresses. OST1, whose encoding gene is expressed specifically in guard cells, not only acts upstream of reactive oxygen species production but also regulates ABA-induced stomatal closure by phosphorylating both the anion and cation channels SLOW ANION CHANNEL-ASSOCIATED 1 (SLAC1) and POTASSIUM CHANNEL IN ARABIDOPSIS THALIANA 1 (KAT1). ABA- and drought-induced stomatal closure are strongly impaired in Arabidopsis (*Arabidopsis thaliana*) *ost1* mutants (Mustilli et al., 2002; Yoshida et al., 2002; Geiger et al., 2009; Lee et al., 2009; Sato et al., 2009). *ost1* single mutants show no obvious developmental phenotypes other than impaired stomatal movement. Due to functional redundancy between SnRK2.2, SnRK2.3, and SnRK2.6, the *Atsnrk2.2 snrk2.3 snrk2.6* triple mutant displays extreme insensitivity to ABA (Nakashima et al., 2009). The triple mutant also exhibits a substantial reduction in its tolerance to drought that accompanies the suppression of ABA- and osmotic stress-induced genes with conserved ABA-responsive elements (ABREs) in their promoters (Fujii et al., 2009; Fujii and Zhu, 2009). However, OST1 function remains elusive in other plant species.

Tomato (*Solanum lycopersicum*) is one of the most common vegetable crops worldwide, with high economic value. About 180 million tons of tomatoes are produced each year, but not all varieties are suited to resist stress or for consumption (Rothan et al., 2019). Flowering is one of the most essential phenological stages in tomato plants as it reflects the transition from vegetative to reproductive development (Lifschitz and Eshed, 2006; Silva et al., 2019). This floral transition is complex and precisely regulated by internal and external signals (Tsuji et al., 2011; Song et al., 2013). In Arabidopsis, several key flowering integrators have been identified, including *FLOWERING LOCUS T* (*FT*), *SUPPRESSOR OF OVEREXPRESSION OF CONSTANS 1* (*SOC1*), and *AGAMOUS-LIKE 24* (Yu et al., 2002; Helliwell et al., 2006; Navarro et al., 2011). The *FT* orthologs *SINGLE FLOWER TRUSS* (*SFT*) and *SELF PRUNING 5G* (*SP5G*) play dominant roles in controlling flowering transition of the day-neutral tomato plant (Molinero-Rosales et al., 2004; Lifschitz et al., 2006; Krieger et al., 2010; Soyk et al., 2017). Only a few TFs

regulate *SFT* or *SP5G* expression (Weng et al., 2016; Cui et al., 2020). Abiotic stresses also substantially affect flowering time (Takeno, 2016). In several plant species, flowering time is accelerated upon drought stress, shortening the life cycle, a process known as drought escape (DE; Sherrard and Maherali, 2006; Franks et al., 2007; Riboni et al., 2013; Shavrukov et al., 2017; Du et al., 2018). ABA is also involved in DE responses, as it induces *FT* and *SOC1* transcription in Arabidopsis (Martignago et al., 2020). The *Atsnrk2.2 snrk2.3 snrk2.6* triple mutant is early-flowering relative to its wild-type (WT; Wang et al., 2013). However, the basis for this effect in Arabidopsis is not clear, and whether tomato plants display a similar phenotype is uncertain, underscoring the need to explore the relationship between drought stress responses and flowering in tomato.

In this work, we report that loss of function of SlOST1 results in drought hypersensitivity and late flowering under both normal and drought stress conditions. We conducted phosphoproteomics analyses and determined that SlOST1 directly interacts with and phosphorylates the TF VASCULAR PLANT ONE-ZINC FINGER 1 (SlVOZ1). Furthermore, ABA treatment enhanced the phosphorylation, protein stability and nuclear translocation of SlVOZ1, suggesting the critical role of ABA in regulating SlOST1-mediated flowering under drought treatment. VOZ-type TFs play roles in flowering as well as biotic and abiotic stress responses (Nakai et al., 2013a, 2013b; Prasad et al., 2018; Schwarzenbacher et al., 2020). Using DNA affinity purification sequencing (DAP-seq), we identified five primary SlVOZ1 binding motifs, four of which were unknown. The *SFT* promoter contained multiple SlVOZ1 binding motifs. We also showed that SlVOZ1 directly binds to the *SFT* promoter to stimulate tomato flowering in response to drought stress. Collectively, our work indicates that the SlOST1–SlVOZ1 module may play an essential role in balancing drought stress responses and flowering transition in tomato.

Results

Phylogenetic analysis of tomato OST1 and generation of *slost1* mutant alleles by CRISPR/Cas9 editing

Although its Arabidopsis counterpart is a key protein kinase in plant response to abiotic stress, the biological function of tomato OST1 remains largely obscure. We extracted the predicted protein sequences from all *SlSnRK2* genes in the tomato genome (ITAG2.4), using Arabidopsis SnRK2s as queries by BLAST search (Figure 1A). We identified eight tomato genes as likely homologs of Arabidopsis *SnRK2* genes. In particular, Solyc01g108280 was highly similar to Arabidopsis *OST1* (*AtOST1*) and corresponded to *SlOST1*, encoding a protein of 362 amino acids sharing over 85% identity with AtOST1 (Figure 1B). Transient infiltration of a *SlOST1-yellow fluorescent protein* (*YFP*) construct in *Nicotiana benthamiana* leaves revealed that SlOST1 mainly localizes to the cytoplasm and the nucleus, similar to the *35S:YFP* control (Supplemental Figure S1A). Using publicly available transcriptome data, we determined that *SlOST1* is highly expressed in leaves, buds and fruits of different stages (Supplemental Figure S1B).

We designed two single-guide RNAs (sgRNAs) targeting the first and second exons of *SlOST1*, respectively, to edit the gene in two tomato genetic backgrounds: the cultivars Micro Tom (MT) and Ailsa Craig (AC; LA2838A) using clustered regularly interspaced short palindromic repeats (CRISPR)–CRISPR-associated protein 9 (Cas9; Figure 1C). After screening tomato transformants, we isolated two mutant alleles in the MT background harboring 22-bp (*slost1-1*) or 220-bp (*slost1-2*) deletions at the target sequence. We also identified two *slost1* mutant lines in the AC background with 2-bp (*slost1-3*) or 5-bp (*slost1-4*) deletions. The sequence alignment of these four CRISPR alleles is presented in Supplemental Figure S2A in detail. To check for potential off-target effects arising from genome editing, we compared the genomic sequences between *SlOST1* and other tomato *SnRK2* genes. As shown in Supplemental Figure S2B, *SnRK2*s and *SlOST1* did not share sequence similarities around the sgRNA target sites.

Mutations in *SlOST1* attenuate drought tolerance

Since OST1 is crucial in regulating stomatal movement as well as contributing to drought stress responses (Mustilli et al., 2002), we evaluated the drought tolerance phenotype of the *slost1* mutants. We withheld water for about 7 days, after which two *slost1* mutant alleles started to display severe signs of leaf curling and wilting compared to their WT. After re-watering, the WT recovered and survived, whereas the *slost1* mutants did not (Supplemental Figure S3A). We measured the water loss rate (WLR) of detached leaves as another indicator of drought tolerance. We recorded a higher WLR in the detached leaves of the two *slost1* mutants (*slost1-1* and *slost1-2*) tested compared to their WT (Supplemental Figure S3B). Plants with greater leaf evaporation due to open stomata exhibit a lower leaf surface temperature, which can be assessed by far-infrared imaging. The leaf temperature of *slost1* mutants was lower than that of the WT under normal growth conditions (Supplemental Figure S3C). These results highlighted the conserved functions of SlOST1 in mediating drought responses in tomato.

SlOST1 positively regulates flowering transition

We also characterized developmental phenotypes associated with growth and flowering time of *slost1* mutants. The *slost1* alleles *slost1-1* and *slost1-2* (MT background) flowered later than their corresponding WT when grown under long-day (LD) conditions, as indicated by the greater number of leaves produced before the emergence of the primary inflorescence (Figure 1D). Consistent with this observation, *slost1-3* and *slost1-4* (AC background) mutant alleles also showed a later flowering phenotype than their WT, based on leaf number under both LD and short-day (SD) conditions (Figure 1E), indicating that SlOST1 is involved in regulating floral transition.

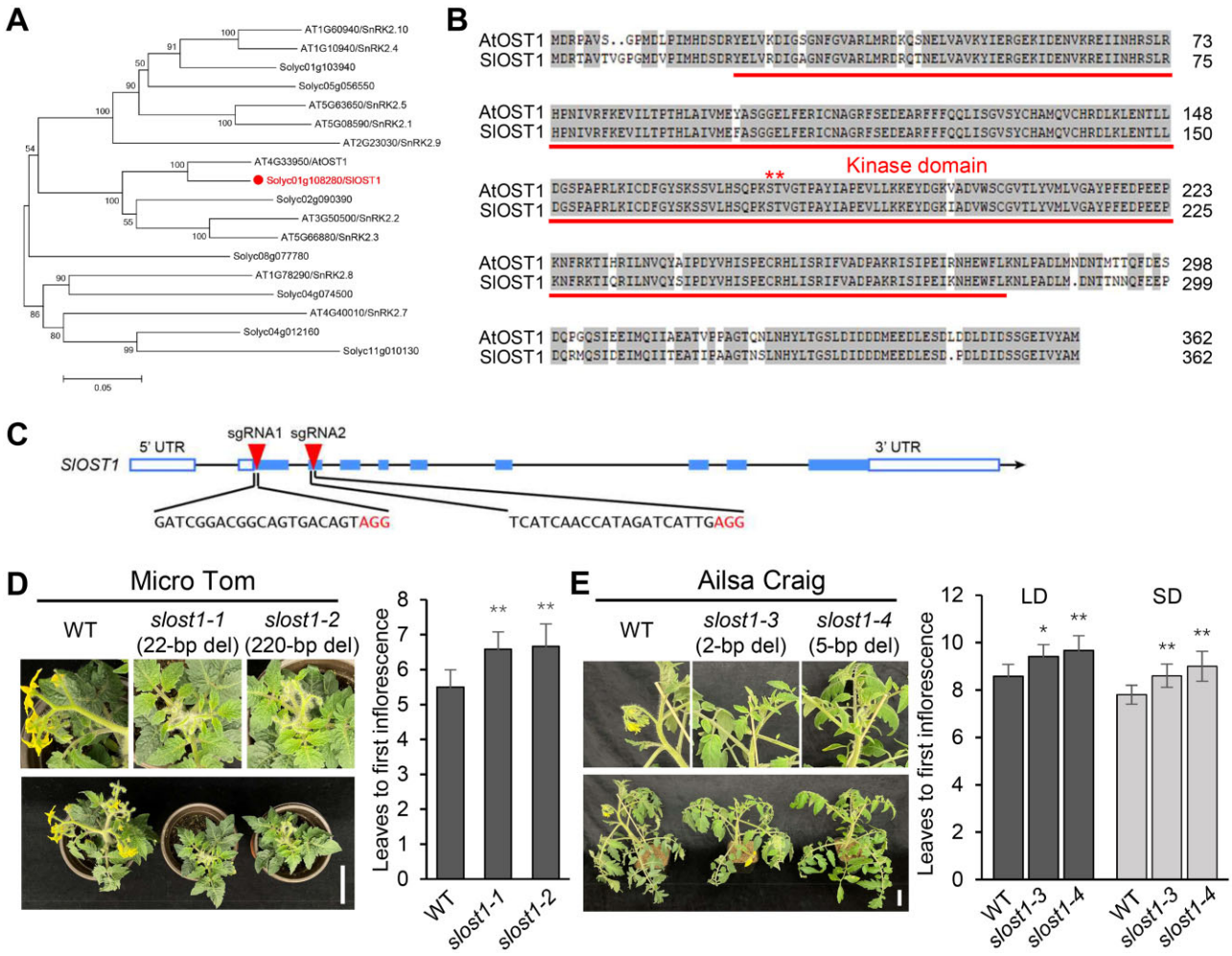

Figure 1 OST1 regulates flowering transition in tomato. A, Phylogenetic analysis of SnRK2 proteins from Arabidopsis and tomato, generated in MEGA 7 with the neighbor-joining method. B, Protein sequence alignment of SlOST1 and AtOST1. Red asterisks indicate the conserved amino acids required for OST1 kinase activity. C, Schematic diagram of the two sgRNAs designed to specifically edit *SlOST1* in two tomato genetic backgrounds, MT and AC, by CRISPR–Cas9. D, Delayed flowering of *slost1* mutants compared to WT plants (MT) under LD conditions. Data represent mean ± standard deviation (SD, $n = 6$). E, Late flowering of *slost1* mutants compared to WT plants (AC) under LD and SD conditions. Data represent mean ± SD ($n = 6$). *$P < 0.05$, **$P < 0.01$, Student's t test relative to WT. Scale bars, 5 cm.

SlOST1 physically interacts with and phosphorylates SlVOZ1

We recently developed an effective phosphoproteomics approach to study putative substrates of protein kinases including SlOST1 in tomato (Hsu et al., 2018). We selected several TFs identified from this methodology and investigated their potential interaction with and phosphorylation by SlOST1, which revealed SlVOZ1 as a putative substrate for the kinase. SlVOZ1 shared high sequence similarity with its Arabidopsis counterpart AtVOZ1 (Supplemental Figure S4). Public transcriptome data indicated that *SlVOZ1* is highly expressed in tomato leaves, roots, flower tissues and fruits (Supplemental Figure S5). Our phosphoproteomics data also identified the putative phosphorylation site in SlVOZ1 as serine 67 (S67). We introduced a point mutation in the *SlVOZ1* coding sequence that resulted in a change from S67 to the nonphosphorylatable residue alanine (A67). Upon incubation with recombinant glutathione S-transferase (GST) fused to SlOST1 (GST-SlOST1), GST-SlVOZ1^{S67A} showed an almost complete loss of phosphorylation during in vitro kinase assays, confirming S67 as the key residue phosphorylated by SlOST1 in SlVOZ1 (Figure 2A). Moreover, a Phos-Tag assay demonstrated a shift in mobility for SlVOZ1 in the presence of SlOST1 in a dose-dependent manner, suggesting that SlOST1 is required for the phosphorylation of SlVOZ1 (Figure 2B).

We used split-luciferase (LUC) assays to validate the direct interaction between SlOST1 and SlVOZ1 in vivo. LUC complementation imaging (LCI) assays resulted in strong LUC activity when *N. benthamiana* leaves were co-infiltrated with *SlOST1-cLUC* and *SlVOZ1-nLUC* constructs, while we detected no LUC activity from the co-infiltration of negative controls (Figure 2C). We confirmed this interaction by conducting co-immunoprecipitation (Co-IP) assays in protoplasts co-transfected with constructs encoding SlVOZ1-MYC and SlOST1-HA when using anti-HA agarose antibodies

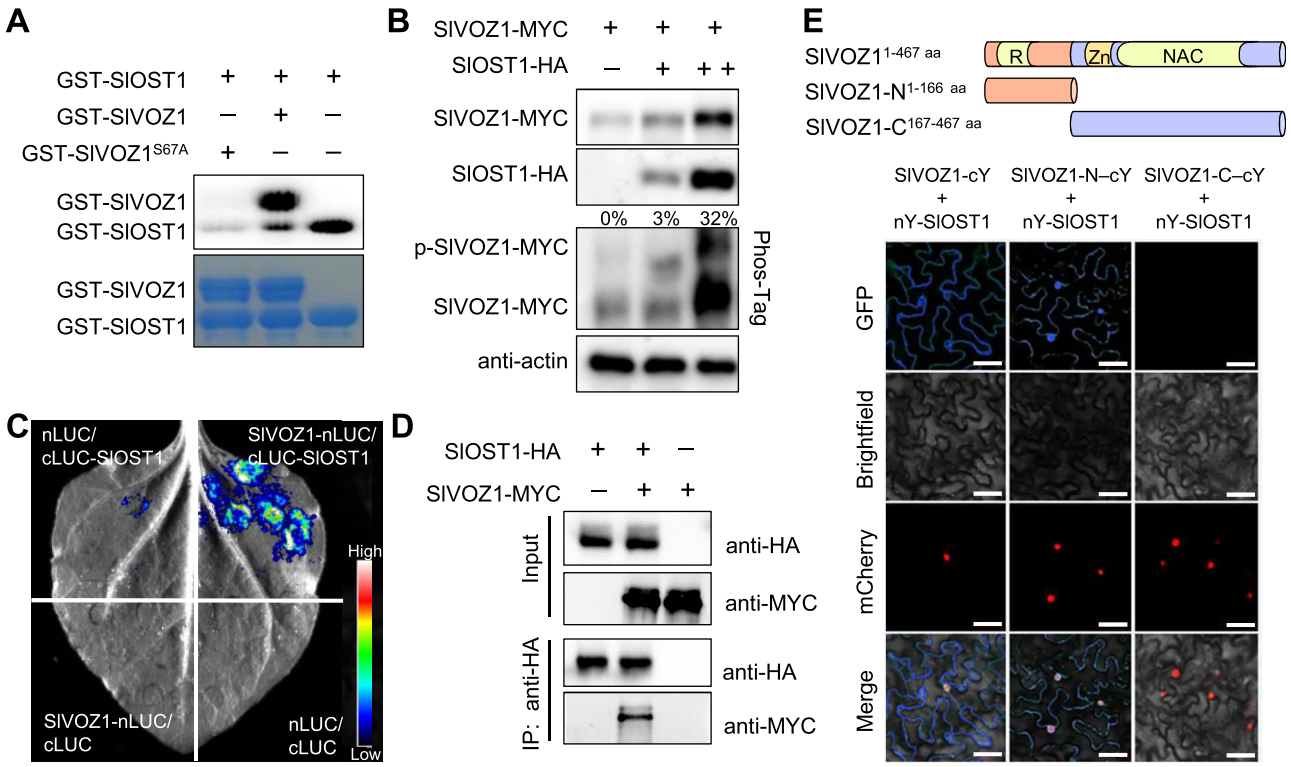

Figure 2 SlOST1 physically interacts with and phosphorylates SlVOZ1. A, SlOST1 phosphorylates SlVOZ1 in vitro. Recombinant purified GST-SlOST1 was incubated with GST-SlVOZ1 or GST-SlVOZ1^{S67A} in kinase reaction buffer. The proteins were separated by SDS–PAGE. Top, autoradiogram; bottom, Coomassie Brilliant Blue staining. B, Phosphorylation of SlVOZ1 by SlOST1 in transfected Arabidopsis protoplasts. *SlVOZ1-MYC* was co-transfected alone or with increasing amounts of *SlOST1-HA* plasmid DNA in protoplasts. Protein abundance and mobility shift were detected by immunoblot and Phos-Tag assay, respectively. The ratio of p-SlVOZ1 to SlVOZ1 is shown. C, LCI assay showing the physical interaction between SlOST1 and SlVOZ1. D, Co-IP assay demonstrating the interaction between SlOST1 and SlVOZ1 in protoplasts. SlOST1-HA was precipitated with anti-HA agarose. SlOST1 and SlVOZ1 proteins were separated by immunoblot and detected with anti-HA and anti-MYC antibodies, respectively. E, BiFC assay in *N. benthamiana* leaves showing the specific interaction between SlOST1 and SlVOZ1. Schematic diagrams indicate the various constructs encoding full-length or truncated SlVOZ1 fused to cYFP; SlOST1 was fused to nYFP. *H2B-mcherry* was co-infiltrated as a nuclear marker. Scale bars, 50 μm.

(Figure 2D). To determine where in the cell SlOST1 and SlVOZ1 interact, we performed bimolecular fluorescence complementation (BiFC) experiments. The co-infiltration of *N. benthamiana* leaves with full-length *SlVOZ1-cYFP* and *SlOST1-nYFP* constructs led to a strong YFP signal in the cytoplasm (Figure 2E). We observed YFP signals in both the cytoplasm and the nucleus when co-infiltrating *SlOST1-nYFP* and a construct encoding the first 166 amino acids of SlVOZ1 fused to cYFP. In contrast, the co-infiltration of *SlOST1-nYFP* with a construct encoding amino acids 167–467 of SlVOZ1 fused to cYFP did not reconstitute YFP, indicating that the N terminus of SlVOZ1 (containing the transcriptional regulatory domain) is essential for the SlOST1–SlVOZ1 interaction.

SlOST1 enhances the protein stability of SlVOZ1

To understand how SlOST1 influences the function of SlVOZ1, we employed an in vitro cell-free degradation assay to examine SlVOZ1 protein stability in the presence of SlOST1. We observed rapid protein degradation when both GST-SlVOZ1 and GST-SlVOZ1^{S67A} recombinant proteins were incubated with total protein extracts prepared from WT tomato plants (Figure 3A). However, co-incubation with recombinant GST-SlOST1 suppressed the degradation of SlVOZ1, as did treatment with the 26S proteasome inhibitor MG132. SlVOZ1^{S67A} remained susceptible to degradation even in the presence of recombinant GST-SlOST1 (Figure 3A), suggesting that phosphorylation of SlVOZ1 at S67 is critical for SlVOZ1 protein stability. We also tested SlVOZ1 protein stability in a transient protoplast system. We detected a low abundance of SlVOZ1 when protoplasts were transfected with a *SlVOZ1* construct alone; however, SlVOZ1 accumulated to higher levels when protoplasts were co-transfected with *SlOST1* or treated with MG132. SlVOZ1^{S67A} abundance did not change when co-transfecting protoplasts with *SlVOZ1*^{S67A} and *SlOST1* constructs (Figure 3B), in agreement with the results from the in vitro cell-degradation assay. Furthermore, we determined SlVOZ1 protein levels in the WT and *slost1* mutants to assess whether SlOST1 is required in planta for SlVOZ1 protein stability. To this end, we generated a specific antibody raised against recombinant SlVOZ1. We confirmed the specificity

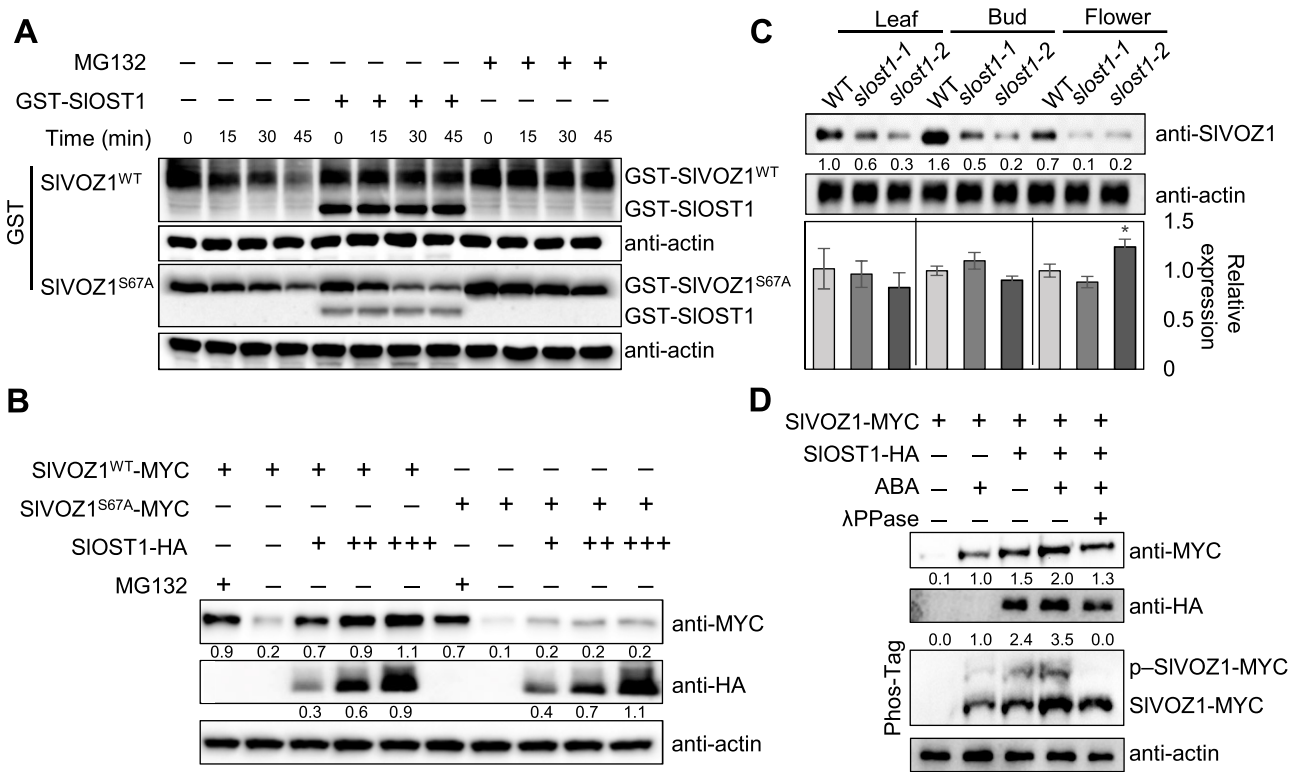

Figure 3 SlOST1 promotes the protein stability of SlVOZ1. A, In vitro cell-free degradation assay showing the effects of SlOST1 on SlVOZ1 and SlVOZ1^{S67A} degradation. Equal amounts of recombinant GST-SlOST1, GST-SlVOZ1, or GST-SlVOZ1^{S67A} proteins were incubated with total protein extracts from WT tomato seedlings for 15, 30, and 45 min without or with 10-μM MG132 added. SlOST1 and SlVOZ1 proteins were detected with anti-GST antibody. Actin served as a loading control. B, SlVOZ1 protein stability is enhanced by SlOST1 in protoplasts. An equal amount of *SlVOZ1-MYC*, *SlVOZ1^{S67A}-MYC*, and *SlOST1-HA* (in an increasing concentration) plasmid DNA was co-transfected in protoplasts. SlOST1, SlVOZ1, and SlVOZ1^{S67A}-MYC protein abundance as determined by immunoblot. Actin served as a loading control. C, SlVOZ1 protein abundance and *SlVOZ1* transcript levels in WT and *slost1* mutants. Total proteins from different tissues were extracted from 9-week-old tomato plants and were probed with anti-SlVOZ1 antibody. Protein levels were quantified using ImageJ. The gene expression data were normalized to WT and represent means ± SD from three biological replicates. D, ABA enhances the protein stability and phosphorylation of SlVOZ1. The *SlVOZ1* construct was transfected alone or with *SlOST1* in protoplasts treated with ABA. The protein stability and phosphorylation of SlVOZ1 were determined by immunoblot and Phos-Tag, respectively. λPPase treatment was applied to abolish the phosphorylation of SlVOZ1.

of the anti-SlVOZ1 antibody against recombinant GST-SlVOZ1; the antibody did not recognize GST-SlVOZ2, a GST fusion to the related TF SlVOZ2. The SlVOZ1 antibody recognized a band of the expected molecular weight for SlVOZ1 in WT protein extracts, but not in *slvoz1* mutants (Supplemental Figure S6). SlVOZ1 protein levels were lower in the *slost1* mutant lines relative to the WT in leaves, buds, and flower tissues (Figure 3C). Reverse transcription–quantitative PCR (RT–qPCR) analysis revealed that *SlVOZ1* expression is comparable in the WT and *slost1* mutants (Figure 3C), indicating that SlOST1 regulates SlVOZ1 mainly at the posttranscriptional level.

Given that Arabidopsis OST1 kinase activity is activated by ABA and abiotic stress, we tested the effects of ABA treatment on the regulation of SlOST1-mediated phosphorylation and protein stability of SlVOZ1. We performed in-gel kinase activity assays to confirm that SlOST1 activity is activated by ABA in tomato (Supplemental Figure S7). We also transiently transfected protoplasts with a *SlVOZ1* construct, alone or together with *SlOST1* and incubated them with ABA, which enhanced SlVOZ1 protein stability and increased its phosphorylation status mediated by SlOST1, as indicated by a mobility shift. Treatment with λ phosphatase (λPPase) eliminated such phosphorylation (Figure 3D), suggesting that ABA plays an important role in regulating SlOST1-mediated phosphorylation and stability of SlVOZ1.

SlOST1 promotes the nuclear translocation of SlVOZ1

Arabidopsis VOZ1 primarily localizes in the cytoplasm and its translocation to the nucleus upon stimulation is essential for its functions (Selote et al., 2018). We investigated the subcellular localization of SlVOZ1 as well as the potential effects of SlOST1 and ABA upon its localization pattern. We transiently co-infiltrated *SlVOZ1-GFP* and the nuclear localization marker *H2B-mCherry* (encoding a fusion protein between histone H2B and mCherry) in *N. benthamiana* leaves, which revealed a primarily cytosolic localization for SlVOZ1, in agreement with previous studies (Supplemental Figure S8). A fraction of SlVOZ1-GFP accumulated in the nucleus when *SlVOZ1-GFP* was co-infiltrated with *SlOST1* and the leaves were treated with

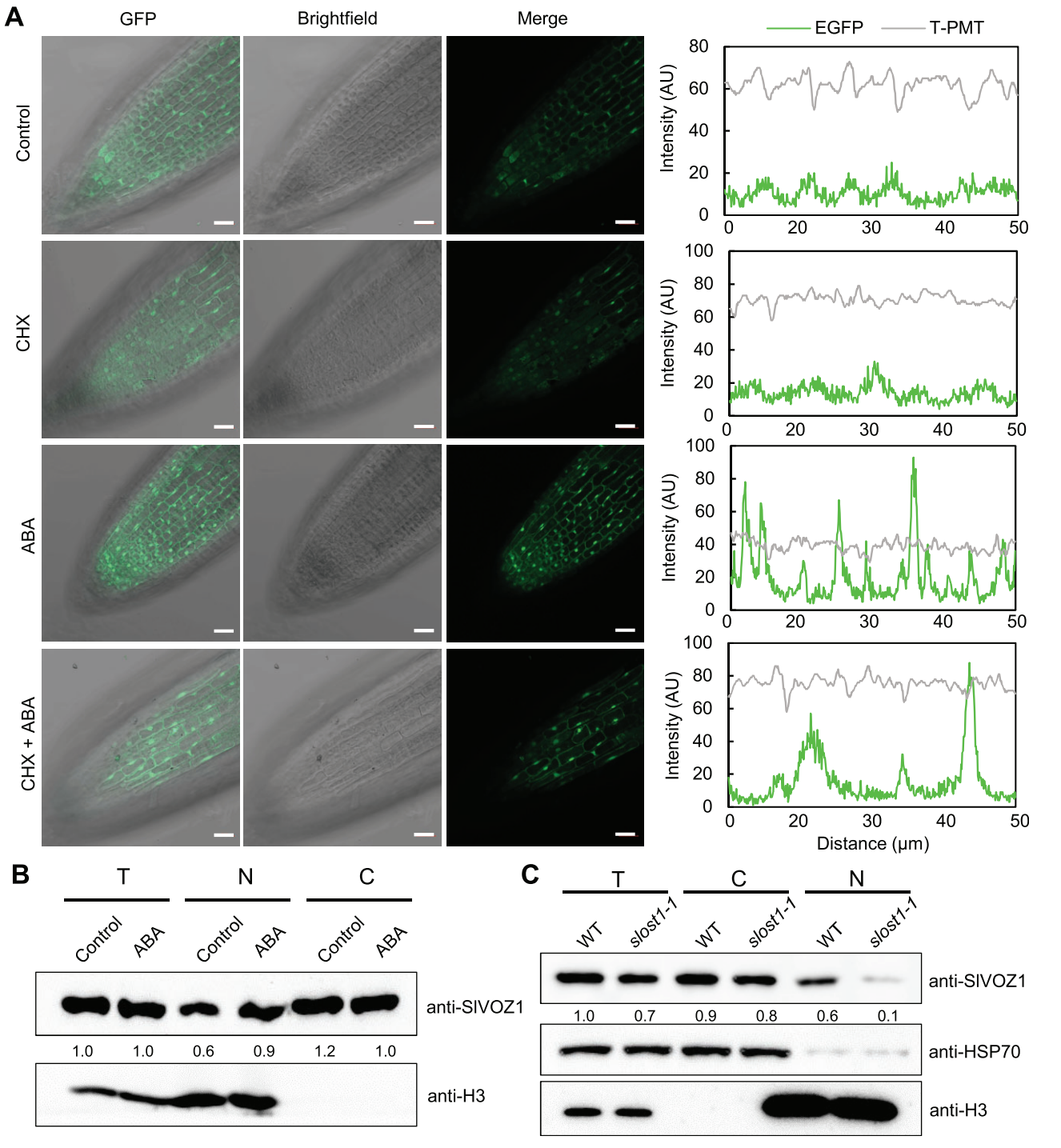

Figure 4 SlOST1 regulates the nuclear translocation of SlVOZ1. A, Representative images showing the subcellular localization of SlVOZ1 with or without ABA and CHX treatments. Four-day-old *SlVOZ1-GFP* transgenic Arabidopsis seedlings were treated with liquid MS medium without or with ABA and CHX before observing GFP fluorescence by confocal microscopy. The GFP intensity in the selected root region was quantified by ZEN version 3.2 software. Scale bars, 50 μm. B, Immunoblot results showing the nuclear accumulation of SlVOZ1 after ABA treatment. Seven-day-old *SlVOZ1-GFP* transgenic Arabidopsis seedlings were treated with 50-μM ABA for 3 h before harvest. The accumulation of SlVOZ1 and nuclear proteins were detected by anti-SlVOZ1 and anti-H3 antibodies, respectively. C, Immunoblot assay showing the accumulation of SlVOZ1 in WT and *slost1* mutants. T, total protein; C, cytosolic protein; and N, nuclear proteins isolated from 7-day-old tomato seedlings using the CelLytic PN extraction kit. The abundance of SlVOZ1 was detected with anti-SlVOZ1 antibody; cytosolic and nuclear proteins were detected with anti-HSP70 and anti-H3 antibodies, respectively.

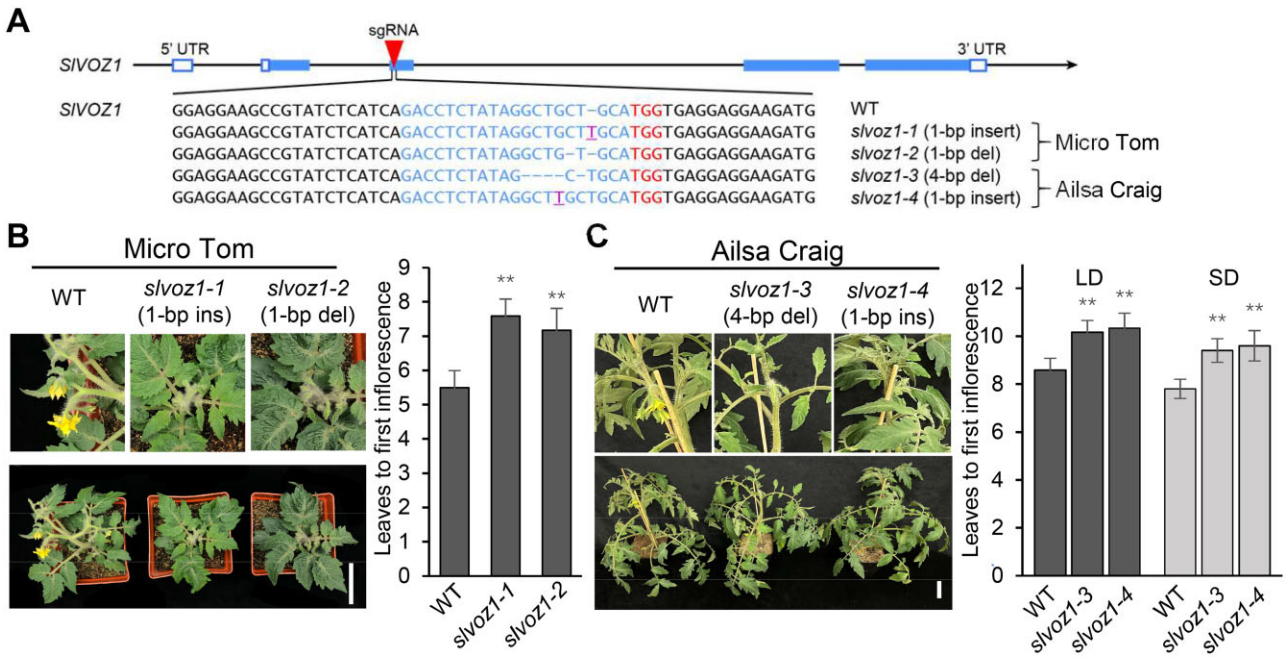

Figure 5 SlVOZ1 is essential for the flowering transition in tomato. A, Schematic diagrams of the sgRNA designed to target *SlVOZ1* with CRISPR–Cas9 and independent CRISPR alleles created in the MT and AC backgrounds. B, Flowering phenotype in WT and *slvoz1* mutants (MT background) under LD conditions. Data represent mean ± SD ($n = 6$). C, The *slvoz1* mutants are late flowering (AC background), as determined by leaf number under LD and SD conditions. Data represent mean ± SD ($n = 6$). $^{**}P < 0.01$, Student's *t* test, relative to WT. Scale bars, 5 cm.

ABA. In contrast, the *SlVOZ1*^{S67A}*-GFP* construct only showed fluorescence in the cytoplasm, even when co-infiltrated with *SlOST1* and with ABA treatment (Supplemental Figure S8), suggesting that ABA and SlOST1 are required for the nuclear translocation of SlVOZ1. In a complementary approach using transgenic Arabidopsis plants expressing *SlVOZ1-GFP*, we mainly detected SlVOZ1-GFP fluorescence in the cytoplasm of root cells under control conditions, but ABA treatment enhanced accumulation of SlVOZ1-GFP in the nucleus (Figure 4A). To test whether the nuclear accumulation of SlVOZ1 was due to translocation from the cytoplasm to the nucleus, we treated *SlVOZ1-GFP* transgenic Arabidopsis seedlings with ABA and the protein biosynthesis inhibitor cycloheximide (CHX). Even under these conditions, we observed the relocation of SlVOZ1-GFP to the nucleus upon ABA treatment, demonstrating that existing SlVOZ1-GFP rather than newly translated SlVOZ1-GFP relocates to the nucleus upon phytohormone stimulus (Figure 4A). We independently confirmed these observations by cell fractionation assays, whereby we separated Arabidopsis protein extracts into cytosolic and nuclear fractions. ABA treatment increased the abundance of SlVOZ1 in the nuclear fraction from *SlVOZ1-GFP* transgenic seedlings (Figure 4B). In addition, SlVOZ1 protein levels decreased in total protein extracts from *slost1* mutants compared to the WT, although the cytosolic pool of SlVOZ1 accumulated to comparable levels in the WT and *slost1* mutants. The nuclear abundance of SlVOZ1 was much lower in *slost1* mutants relative to their WT (Figure 4C).

SlVOZ1 is essential for flowering transition in tomato

Arabidopsis VOZ1 and VOZ2 redundantly regulate flowering time (Mimida et al., 2011; Yasui et al., 2012; Celesnik et al., 2013), prompting us to explore the role of *SlVOZ1* in regulating tomato flowering. We generated *slvoz1* mutants in the MT and AC backgrounds using CRISPR/Cas9. As illustrated in Figure 5A, we isolated two independent *slvoz1* alleles (*slvoz1-1* and *slvoz1-2*) in the MT background and two *slvoz1* alleles (*slvoz1-3* and *slvoz1-4*) in the AC background. Under LD growth conditions, all *slvoz1* mutants generated by genome editing exhibited late flowering phenotypes compared to their respective WT (Figure 5, B and C) as indicated by increased leaf number before the emergence of the primary inflorescence. We also observed delayed flowering and a greater leaf number for *slvoz1* mutants (AC background) under SD conditions (Figure 5C). These results indicated that SlVOZ1 plays a positive role in regulating tomato flowering transition.

The SlOST1–SlVOZ1 module is essential for drought-accelerated flowering

Drought-accelerated flowering, also known as a DE response, has been reported in several plant species (Franks, 2011; Du et al., 2018), but whether it is conserved in tomato remains to be explored. We examined the mannitol response, leaf surface temperature, and WLR of *slvoz1* mutants, which are three phenotypes that reflect the extent of drought tolerance. Both *slvoz1* and *slost1* mutants appeared hypersensitive to growth on medium containing mannitol compared

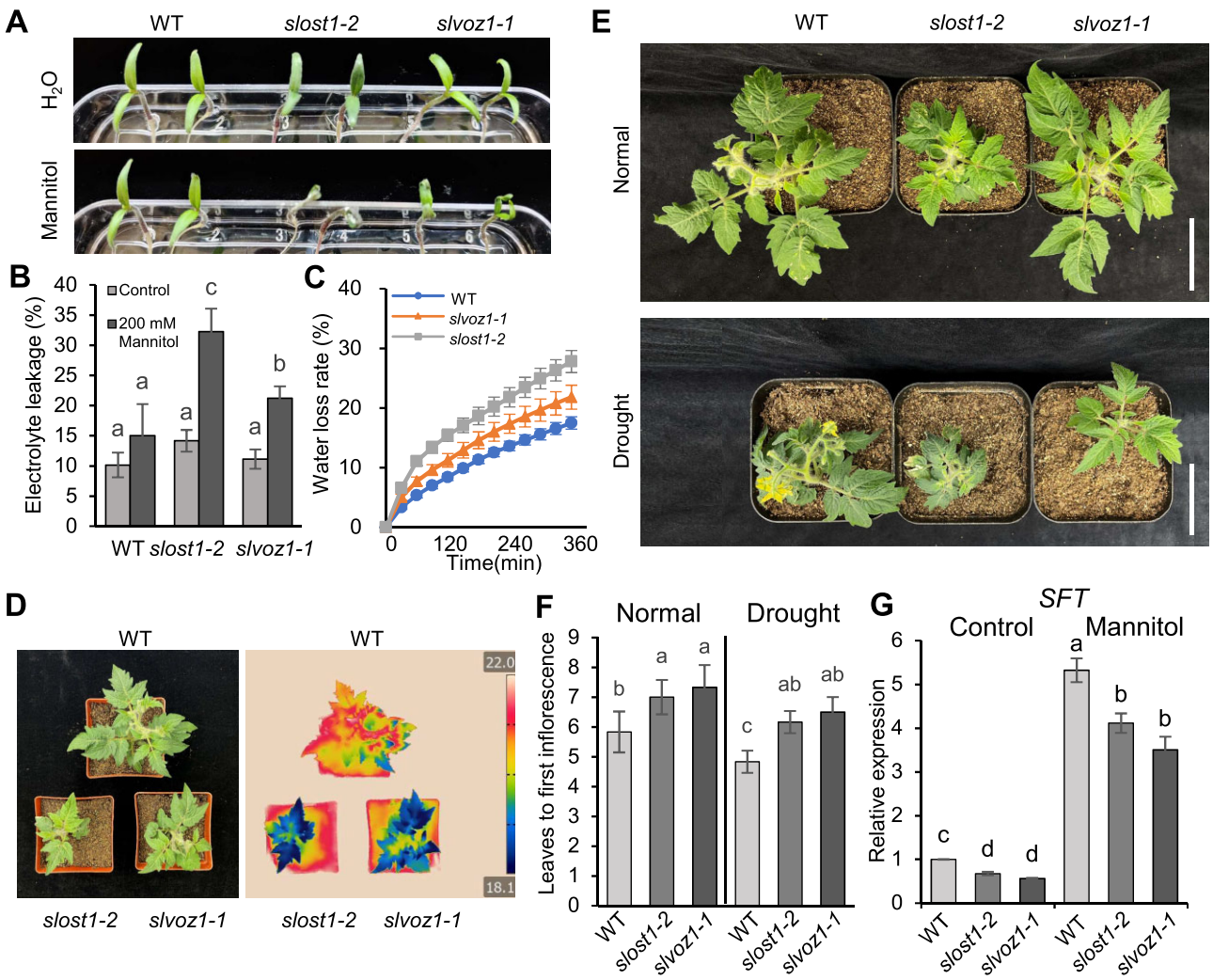

Figure 6 Drought-accelerated flowering is partially dependent on the SlOST1–SlVOZ1 module. A and B, Representative phenotypes and electrolyte leakage of WT, *slost1* and *slvoz1* mutants (MT background) under control (H_2O) and 200-mM mannitol treatment conditions. Data are means ± SD of three biological replicates. Different letters indicate significant differences by two-way ANOVA (Analysis of Variance) (Duncan's multiple range test, $P < 0.05$). C, WLR of WT, *slost1* and *slvoz1* mutants. Data are means ± SD of three biological replicates. D, False-colored infrared-thermal images of the WT, *slvoz1* and *slost1* mutant plants. E, Flowering phenotype of WT, *slost1* and *slvoz1* mutants (MT background) under normal and drought treatment conditions. Scale bars, 5 cm. F, Flowering time of WT, *slost1* and *slvoz1* mutants under normal and drought treatment conditions. Data represent mean ± SD ($n = 6$), and experiments were repeated 3 times independently with similar results. G, Relative *SFT* transcript levels in 18-day-old WT, *slost1*, *slvoz1* seedlings under control and mannitol treatment conditions. Tomato *Actin 7* was used as a reference control. Data represent mean ± SD from three technical replicates. Different letters represent significant differences, as determined using two-way ANOVA with Tukey's post hoc test ($P < 0.05$).

to WT (Figure 6A). Consistently, mannitol-induced electrolyte leakage was higher in the mutants relative to the WT (Figure 6B). Moreover, WLR was faster in the *slvoz1-1* and *slost1-2* mutants than in the WT, likely due to their lower leaf temperature (Figure 6, C and D). Both *slvoz1* and *slost1* mutants were also insensitive to ABA treatment relative to WT, as indicated by seed germination rates (Supplemental Figure S9), indicating that SlVOZ1 is likely involved in ABA signaling and drought response. We also subjected the WT, *slost1* and *slvoz1* mutant plants (MT background) to normal growth conditions or drought treatment. Drought stress suppressed the growth of all genotypes when compared to plants grown under normal irrigation (Figure 6E). As observed in other plant species, the WT flowered earlier after drought treatment, as indicated by flowering time and leaf number, compared to WT plants grown under normal conditions. In contrast, *slost1* and *slvoz1* mutants still exhibited a delayed flowering that was slightly or not affected by drought treatment relative to control conditions (Figure 6, E and F). In fact, the relative flowering time of both mutants was less accelerated by drought treatment compared to WT (Supplemental Figure S10), indicating that drought-accelerated flowering is partially dependent on the SlOST1–SlVOZ1 module in tomato.

We investigated *SFT* expression in *slost1* and *slvoz1* mutants next. Consistent with their delayed flowering

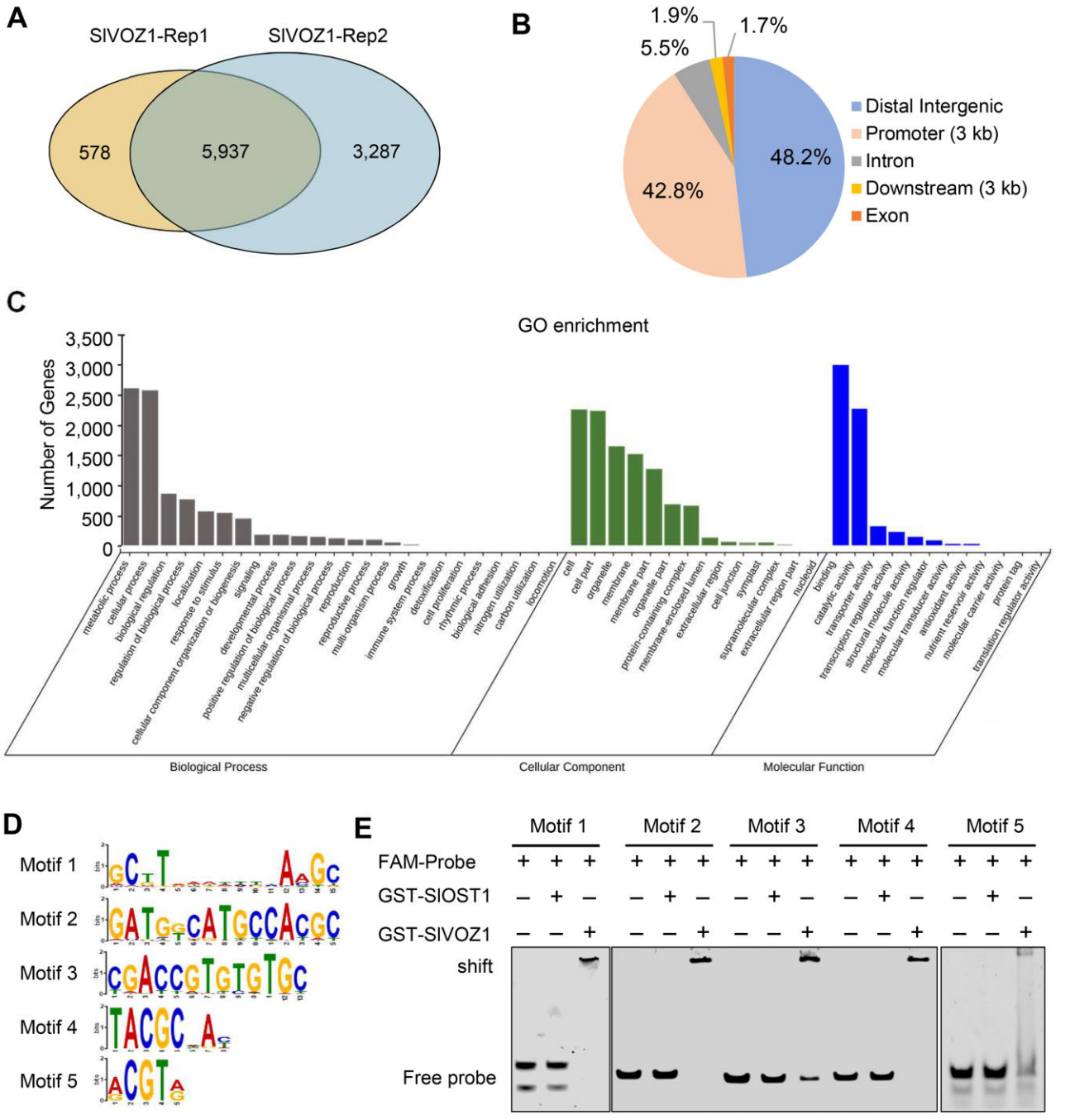

Figure 7 Genome-wide identification of SlVOZ1 binding motifs and target genes by DAP-seq. A, Venn diagram showing the extent of overlap between peaks identified from the two DAP-seq replicates. B, Distribution of high-confidence SlVOZ1 binding peaks along the tomato genome. C, GO enrichment analysis of SlVOZ1 binding peaks. D, The five enriched binding motifs identified for SlVOZ1. E, Validation of the direct binding of SlVOZ1 to the five enriched motifs by EMSA. FAM-labeled DNA probes were incubated with recombinant GST-SlVOZ1 or GST-SlOST1 proteins.

phenotype under normal conditions, *SFT* expression was lower in *slost1* and *slvoz1* mutant plants relative to the WT (Figure 6F; Supplemental Figure S11). *SFT* expression was induced in response to mannitol treatment, supporting the notion that drought stress promotes early flowering in tomato. However, *SFT* expression remained low in *slost1* and *slvoz1* mutants compared to the WT after mannitol treatment (Figure 6G).

Analyses of SlVOZ1 binding sites and target genes in tomato by DAP-seq

In Arabidopsis, the TF VOZ1 primarily associates with promoters that contain the motif GCGT(N)$_7$ACGT (Mitsuda et al., 2004). To identify the potential SlVOZ1 binding motifs and target genes, we performed DAP-seq by incubating recombinant GST-SlVOZ1 with a tomato genomic DNA library, followed by sequencing of VOZ1-bound DNA

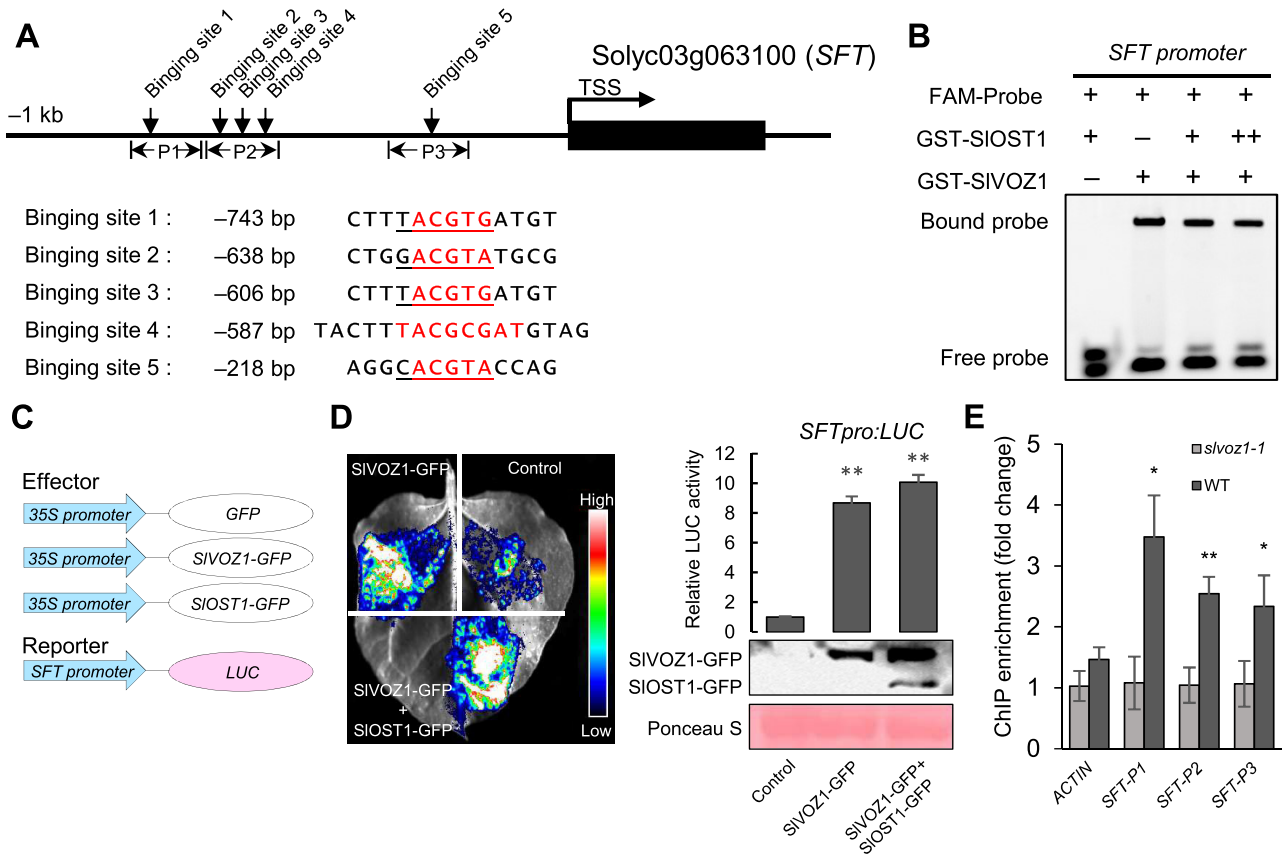

Figure 8 SlVOZ1 directly binds to the *SFT* promoter to activate transcription. A, Illustration of the binding motifs of SlVOZ1 in the *SFT* promoter. B, EMSA showing the direct binding of SlVOZ1 to the *SFT* promoter probes. Recombinant GST-SlVOZ1, GST-SlOST1, or both proteins were incubated with FAM-labeled DNA fragments. C, Schematic diagrams of the effector and reporter constructs used for the transactivation assay. D, Transactivation assay showing that SlVOZ1 activates the transcription of *SFT*. $^{**}P < 0.01$, Student's *t* test, relative to WT. The protein abundance of effectors was detected by immunoblot using anti-GFP antibody. E, ChIP-qPCR assay showing the binding of SlVOZ1 to the *SFT* promoter in vivo. Leaves of 6-week-old tomato plants grown under LD conditions were harvested in the morning for ChIP. Data represent means ± SD of three technical repeats. $^{*}P < 0.05$, $^{**}P < 0.01$, Student's *t* test, relative to WT. Anti-SlVOZ1 antibody was used to precipitate the SlVOZ1–DNA complex in WT and *slvoz1* mutants. ChIP experiments were performed two independent times with similar results.

fragments. We identified 6,515 and 9,224 potential SlVOZ1 target genes from two biological replications, with an overlap of 5,937 genes (Figure 7A; Supplemental Data Sets 1 and 2 and 2). An analysis of their genomic distribution indicated that 43.8% of all peaks are located in promoter regions, with the remaining 46.3% in intergenic regions (Figure 7B). Gene ontology (GO) enrichment analysis established that these putative SlVOZ1 target genes are mainly enriched in cellular processes, metabolic processes, single-organism processes, and response to stimulus, as well as biological regulation (Figure 7C). We identified five major SlVOZ1 binding motifs (Figure 7D). Similar to a previous study in Arabidopsis (Kumar et al., 2018), SlVOZ1 showed preferential binding to promoters containing the motif GC(G/T)T$(N)_7$A(A/C)GC (Motif 1) or GATGGCATGCCACGC (Motif 2), in addition to the new SlVOZ1 binding motifs CGACCGTGTGTGC (Motif 3) and TACGCNAC/T (Motif 4). SlVOZ1 also associated with Motif 5, the ABRE motif (ACGTA/G), which belongs to the G-box family. To confirm the DAP-seq results, we performed electrophoretic mobility shift assay (EMSA). As depicted in Figure 7E, GST-SlVOZ1 but not GST-SlOST1 is directly bound to all five motifs. *SFT* was one of the SlVOZ1 target genes, as determined by DAP-seq analysis.

SlVOZ1 directly binds to the *SFT* promoter to promote its transcription

To unfold the role of SlVOZ1 in flowering regulation, we focused on *SFT*. The *SFT* promoter contained several SlVOZ1 binding motifs (Motifs 4 and 5) (Figure 8A). We performed EMSAs to validate the binding of SlVOZ1 to selected *SFT* promoter probes. Recombinant SlVOZ1, but not SlOST1, showed direct binding to the *SFT* promoter probes in vitro (Figure 8B). Adding SlOST1 to the reactions did not significantly affect the association between SlVOZ1 and its targets. Moreover, we placed the *LUC* reporter gene under the control of the *SFT* promoter (Figure 8C) to determine whether SlVOZ1 directly activated its transcription. Transactivation assays demonstrated that *SFTpro:LUC* activity increased when *SlVOZ1* was co-infiltrated with the *LUC* reporter in *N. benthamiana* leaves relative to the control (reporter only), while *SlOST1* co-infiltration slightly enhanced SlVOZ1-

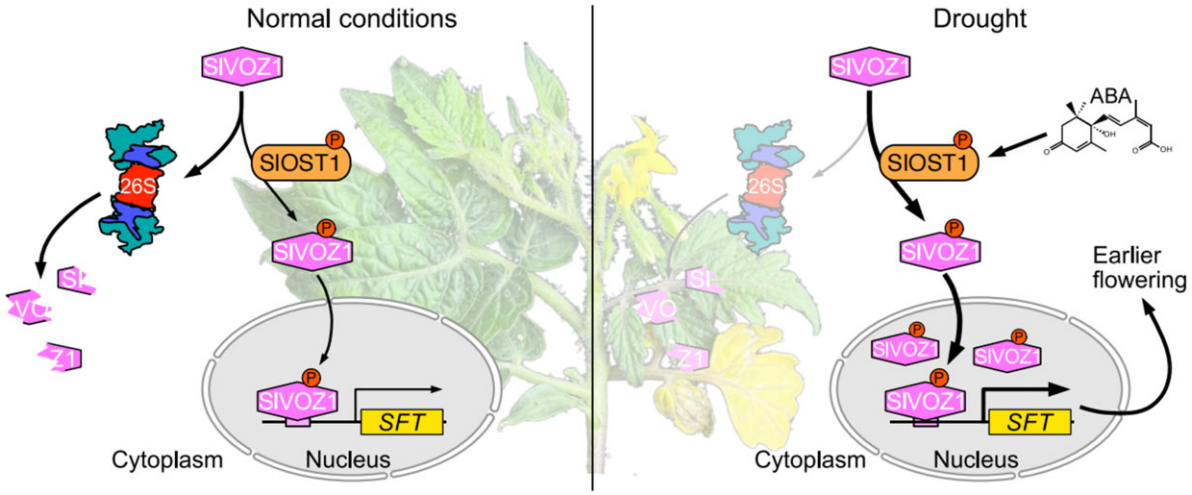

Figure 9 Model illustrating how the SlOST1–SlVOZ1 module balances flowering transition and drought. Upon encountering drought stress, SlOST1 is activated to interact with and phosphorylate SlVOZ1, which leads to enhanced protein stability and nuclear accumulation of SlVOZ1. Nucleus-localized SlVOZ1 then binds to the *SFT* promoter to promote flowering transition in response to drought stress.

mediated *SFT* transcriptional activation. The observed differences were not caused by protein accumulation, as determined by immunoblot analysis of GFP-tagged fusion proteins (Figure 8D). Additionally, we performed a chromatin immunoprecipitation (ChIP) assay using the anti-SlVOZ1 antibody on tomato seedlings to examine the in vivo association of SlVOZ1 with the *SFT* promoter. We detected significant enrichment for different *SFT* promoter regions (as labeled in Figure 8A) in the WT compared to *slvoz1* mutants, confirming that *SFT* is a direct SlVOZ1 target (Figure 8E).

Discussion

Flowering in tomato is a critical developmental stage that can be vulnerable to environmental stresses. Prolonged exposure to an environmental stress such as drought at this stage can result in substantial yield losses. However, the molecular mechanism underlying the balance between drought stress and flowering transition in tomato has yet to be clarified. In this study, we demonstrated that tomato SlOST1 positively regulates not only drought tolerance but also flowering time under drought stress. We discovered that SlOST1 promotes the stability and nuclear translocation of SlVOZ1 via phosphorylation, which is further enhanced by ABA. Nucleus-localized SlVOZ1 then positively induces the expression of *SFT*, thereby offering a probable mechanism for how tomato balances drought responses and flowering.

In Arabidopsis and several other plant species, OST1 is critical to the regulation of ABA signaling, abiotic stress responses, and stomatal movement (Mustilli et al., 2002; Assmann, 2003; Joshi-Saha et al., 2011; Fujita et al., 2013; Zhu, 2016; Ali et al., 2020). However, the role of OST1 during plant development such as flowering has remained elusive. Our work provided several lines of evidence for how SlOST1 positively regulates tomato flowering time in response to drought stress. We observed delayed flowering in the *slost1* mutants, which were also smaller than the WT, suggesting that *SlOST1* may also participate in the regulation of tomato growth and development. Our findings in tomato are different from the early flowering phenotype observed with the Arabidopsis *snrk2.2 snrk2.3 snrk2.6* triple mutant. A possible explanation for this variation is that OST1 may regulate flowering transition in different plant species via distinct mechanisms. Moreover, we suspect that the severe dwarfism seen in the Arabidopsis triple mutant may contribute to its early flowering, although this hypothesis needs to be tested.

We identified SlVOZ1 as a SlOST1 substrate by phosphoproteomics analysis; SlVOZ1 plays a role in flowering and biotic and abiotic stress response in plants. Arabidopsis VOZ1 mainly accumulates in the cytoplasm, but its translocation to the nucleus is crucial for proper function (Selote et al., 2018; Schwarzenbacher et al., 2020). In our study, we also noticed that SlVOZ1 is an unstable cytosolic protein when seedlings are grown under normal conditions. SlVOZ1 became more stable in the presence of SlOST1. Moreover, ABA activates the kinase activity of SlOST1, which further promotes the phosphorylation, protein stability, and nuclear translocation of SlVOZ1, suggesting that ABA plays a vital role in regulating SlVOZ1 function mediated by SlOST1. Our genetic work revealed that *slvoz1* mutants are late flowering, hypersensitive to mannitol, insensitive to ABA and lose water faster when compared to the WT, as also observed with *slost1* mutants, indicating that *SlVOZ1* and *SlOST1* are likely involved in regulating the ABA-mediated drought tolerance in tomato. In addition, *slost1 slvoz1* double mutants also exhibited a late flowering phenotype similar to their single mutants under both normal and drought conditions (Supplemental Figure S12), further suggesting that the SlOST1–SlVOZ1 module likely plays a key role in drought response and flowering. Our DAP-seq analysis identified five conserved SlVOZ1-binding motifs, of which four (Motifs 2–5) have not been reported previously. The *SFT* promoter contained several SlVOZ1 binding sites, including ABRE

(ABA-responsive element) motifs. Although previous studies have demonstrated that *SFT* is the flowering integrator gene in tomato (Lifschitz et al., 2006; Krieger et al., 2010), its roles in stress responses remain unclear. In our present work, we validated *SFT* as a direct SlVOZ1 target. We also established that *SFT* expression is induced by mannitol treatment, indicating that *SFT* may be involved in regulating drought-accelerated flowering in tomato.

Based on the genetic and biochemical evidence presented in this study, we propose a model for the potential role of the SlOST1–SlVOZ1 module in regulating drought-induced flowering (Figure 9). In this model, the TF SlVOZ1 is unstable and susceptible to degradation under normal conditions. When tomato plants are subjected to adverse conditions such as drought, SlOST1 is activated to promote the protein stability, phosphorylation, and nuclear translocation of SlVOZ1, which directly binds to the *SFT* promoter and results in drought-induced flowering. Other flowering gene(s) may also be regulated by the SlOST1–SlVOZ1 module. Increasing evidence suggests that altering flowering time is a beneficial strategy employed by plants to maximize their chances of survival or reproduction under suboptimal growth conditions; our study adds a new layer to our understanding of how an environmental factor can be integrated into the floral pathways of tomato.

Materials and methods

Plant materials and growth conditions

The MT or AC (LA2838A) cultivars were used as the WT in this study. The indicated WT and mutant plants were grown under controlled conditions (LD conditions: 16-h light/8-h dark cycle; SD conditions: 8-h light/16-h dark cycle, at 25°C during the day and 22°C at night under 100–150 $\mu mol \cdot m^{-2} \cdot s^{-1}$ cool-white fluorescent illumination [PHILIPS MASTER TL5 HO 39W/840 SLV/4], 70% humidity).

Sequence alignment

The protein sequences of *A. thaliana* SnRK2s or VOZ1 members were retrieved from The Arabidopsis Information Resource (http://www.arabidopsis.org/). The protein sequences of tomato SnRK2s or VOZ1 members were obtained from Phytozome version 12.1 (https://phytozome.jgi.doe.gov/pz/portal.html). Sequence comparison was conducted using the online tool MAFFT (http://mafft.cbrc.jp/alignment/server/). To generate neighbor-joining phylogenetic trees, MEGA version 7 was used to perform a bootstrap analysis with 1,000 replicates containing the following parameters: p-distance and pairwise deletion (Kumar et al., 2016).

Construction of CRISPR–Cas9 vectors and generation of tomato mutant lines

The CRISPR–Cas9 vectors were constructed as previously described (Mao et al., 2013; Lang et al., 2017). Primers used for construction of CRISPR constructs and screening transgenic plants for gene editing are listed in Supplemental Table S1. After performing transformation of tomato cultivars (MT and AC backgrounds), ~10–15 primary (T_0) transformants were screened for desired editing at the targeted sites. Homozygous lines (Cas9-free) were used for phenotypic analyses. The homozygous CRISPR alleles *slost1-2* and *slvoz1-1* were crossed to generate the *slost1 slvoz1* double mutant.

ABA and stress treatments

For drought survival experiments, ~4-week-old tomato plants were subjected to drought stress. Water was withheld for a period of 5–7 days before recording plant phenotypes in response to drought. The recovery phenotype was documented after allowing plants to recover from drought with watering for 2 days. For ABA treatments, tomato seeds were first surface sterilized with bleach and plated onto Murashige and Skoog (MS) medium with or without 3-μM ABA. Seed germination rates were scored 5 days after release from stratification. For mannitol treatment, the roots of 7-day-old tomato seedlings were immersed in distilled water or a 200-mM mannitol solution for approximately 1–3 h. Electrolyte leakage from young leaves was measured to determine their mannitol tolerance.

To investigate whether drought stress affects the flowering of tomato plants, WT and mutant tomato seeds were sown onto well-watered soil and allowed to grow for ~20 days before being subjected to drought stress. Drought treatment was controlled by adjusting the daily soil water content to ~30% as previously described (Du et al., 2018; Reichardt et al., 2020). Total leaf number before the emergence of the primary inflorescence and flowering time was measured under both normal and drought conditions.

For WLR measurements, leaves from 6-week-old tomato plants were detached and weighed immediately and every 5 min for 400 min. The percentage loss of fresh weight was calculated on the basis of initial weight. Thermal imaging was performed with a ThermaCAMSC1000 infrared camera (FLIR System, Danderyd, Sweden) as described (Chen et al., 2020a, 2020b).

In vitro kinase assay

The coding sequences of *SlOST1*, *SlVOZ1*, and $SlVOZ1^{S67A}$ were amplified from tomato cDNA (MT) with PrimeSTAR Max DNA Polymerase (TaKaRa, Shiga, Japan, R045B) and cloned into pGEX4T-1 vectors. After transformation into BL21 competent cells, recombinant proteins were purified with glutathione agarose resin (GE Healthcare, Chicago, IL, USA). In vitro kinase assays were performed as described (Hou et al., 2016; Zhu et al., 2020). The indicated recombinant proteins were incubated in reaction buffer (25 mM Tris–Cl, pH 7.4, 12 mM $MgCl_2$, 2 mM DTT, 1 μM ATP plus 1 μCi of [γ-^{32}P]ATP) for 30 min at 30°C before boiling in loading buffer. Protein phosphorylation was visualized by autoradiography (Personal Molecular Imager; Bio-Rad Hercules, CA, USA).

Determination of subcellular localization by confocal microscopy

The indicated *GFP* and nuclear marker *H2B-mCherry* plasmids were introduced into Agrobacterium (*Agrobacterium tumefaciens*) strain GV3101 for transient infiltration in *N. benthamiana* leaves. GFP and mCherry fluorescence were observed by confocal microscopy (Zeiss LSM-710) 2 days later.

Co-IP assay

The coding sequences of the indicated genes were cloned into pHBT95-HA and MYC vectors. The maxi-purified plasmids were transiently co-transfected into Arabidopsis protoplasts as described (Zhu et al., 2014; Zhu et al., 2020; Guo et al., 2021). Total proteins were extracted with IP buffer (50-mM Tris–HCl pH 7.5, 150-mM NaCl, 1-mM EDTA (Ethylenediaminetetraacetic acid), 1-mM DTT (Dithiothreitol), 1-mM PMSF (Phenylmethanesulfonyl fluoride), and protease inhibitor cocktail) and the extracts incubated with monoclonal anti-HA agarose (Sigma, St Louis, MO, USA; A2095) for at least 4 h at 4°C. After immunoprecipitation, the agarose was washed at least 4 times with IP buffer before boiling. The proteins were detected by immunoblot using anti-Myc (Abcam, Cambridge, UK; ab9106) and anti-HA antibodies (Abcam; ab9110).

LCI assay

The coding sequences of *SlOST1* and *SlVOZ1* were cloned in-frame with those of *cLUC* and *nLUC*, respectively. The fusion plasmids were then transformed into Agrobacterium strain GV3101 for transient infiltration of *N. benthamiana* leaves. After infiltration, the *N. benthamiana* plants were grown in the light for 2 days. LUC activity was determined on a Tanon (5200 Multi) imaging system.

BiFC assay

Full-length or truncated coding sequences of *SlOST1* and *SlVOZ1* were cloned in-frame with *nYFP* and *cYFP*, respectively. The BiFC plasmids were introduced into Agrobacterium strain GV3101 for transient transformation of *N. benthamiana* leaves. Two days after co-infiltration, the fluorescence from YFP and the nuclear marker H2B-mCherry were assessed by confocal microscopy (Zeiss LSM-710).

Generation of polyclonal anti-SlVOZ1 antibody

The anti-SlVOZ1 polyclonal antibody was raised by Beijing Protein Innovation Co. Ltd, Beijing, China. Recombinant GST-SlVOZ1 protein was produced in *Escherichia coli* and purified before being used as antigen for immunization of rabbits for polyclonal antiserum production. Antigen-affinity purified antibody was used in immunoblots to detect recombinant or endogenous SlVOZ1 abundance in plants.

Cell-free protein degradation assay

Cell-free protein degradation assays were performed as described (Kong et al., 2015) with minor modifications. Total proteins were extracted from the leaves of 5-week-old tomato plants in extraction buffer (25-mM Tris–HCl, pH 7.5, 10-mM NaCl, 10-mM $MgCl_2$, 5-mM DTT, 1-mM PMSF). The indicated recombinant protein and 1-mM ATP were then added to the total protein extracts. After incubation for the indicated time, the samples were separated by SDS–PAGE (Sodium Dodecyl Sulphate-Polyacrylamide Gel Electrophoresis). Protein abundance was determined by immunoblots with anti-GST antibody (Proteintech Group, 66001-2) at a 1: 5,000 (v/v) dilution. Anti-actin antibodies (Sigma; A0840) were used as a loading control at a 1: 5,000 (v/v) dilution.

Protein stability assay in protoplasts

DNA for the relevant plasmids was transfected into protoplasts as previously described (Zhu et al., 2020; Guo et al., 2021). The transfected protoplasts were incubated in W5 solution with or without 10-μM MG132 overnight before total proteins were extracted using protein lysis buffer (50-mM Tris–HCl, pH 7.5, 150-mM NaCl, 0.1% [v/v] Triton X-100, 1-mM EDTA, 1-mM DTT, 1-mM PMSF, and 1× complete protease inhibitor cocktail). Protein abundance was determined by immunoblots with anti-MYC (Abcam; ab9106) or anti-HA antibodies (Abcam; ab9110) at a 1: 5,000 (v/v) dilution. Anti-actin antibodies were used as a loading control at 1:5,000 (v/v) dilution.

EMSA

EMSA was performed as described (Zhu et al., 2020). The promoter fragments of *SFT* with potential VOZ1-binding sites were synthesized and labeled with FAM (Fluorescein) probes (Supplemental Table S1). Sense and antisense primers were annealed by gradual cooling after denaturation at 95°C for 5 min. The purified recombinant SlVOZ protein was incubated with promoter fragments in EMSA binding buffer (20-mM Tris–HCl, pH 7.5,100-mM NaCl, 2-mM $MgCl_2$, 1-mM DTT, 10% [v/v] glycerol) for 30 min at 4°C. The samples were subsequently separated by electrophoresis on 8% (w/v) nondenaturing polyacrylamide gel before visualization on a Tanon 5200 Multi imaging system (Tanon Shanghai, China).

Transient transactivation assay

A 2,000-bp promoter fragment upstream of the *SFT* start codon was cloned into the pGreenII-0800-LUC vector. All effector and reporter constructs were introduced into Agrobacterium strain GV3101. Cultures from the indicated effectors and the *SFTpro-LUC* reporter were co-infiltrated into *N. benthamiana* leaves. After 48 h, *N. benthamiana* leaves were sprayed with (0.3 mg/mL) luciferin and 0.1% (v/v) Triton X-100 before LUC activity was recorded with a CCD camera (Tanon 5200 Multi) as described (Guo et al., 2021).

Cell fractionation assay

Equal amounts of tissues from 1-week-old tomato or Arabidopsis seedlings were collected for cell fractionation assays. The nuclear and cytoplasmic fractions were prepared by using a CelLytic PN Isolation Kit (Sigma) as described (Bao et al., 2014). SlVOZ1 protein was detected with anti-SlVOZ1 antibody at a 1:2,000 (v/v) dilution. Anti-HSP70 (Agrisera, Vännäs, Sweden; AS08 371) and anti-H3 antibodies (Abcam; ab1791) were used as cytoplasmic and nuclear markers at a 1:5,000 (v/v) dilution, respectively.

Phos-tag assay

The phosphorylation of SlVOZ1 was detected by a mobility shift assay consisting of Phos-Tag reagent as described previously (Mao et al., 2011). *SlVOZ1-MYC* was transfected with or without the *SlOST1-HA* construct in Arabidopsis protoplasts before addition of 5-μM ABA for overnight incubation at room temperature (in the dark). Total proteins were extracted and separated on a 10% (v/w) SDS–PAGE gel containing 50-μM Phos-tag (APExBIO) and 100 μM $MnCl_2$. The mobility shift of SlVOZ1 was detected with anti-MYC antibody (Abcam).

In-gel kinase assay

The experiments were performed as previously described (Hou et al., 2016). Ten-day-old tomato seedlings grown on MS medium were treated with water or 50-μM ABA for 1 h. Total proteins were then extracted in lysis buffer (100-mM HEPES, pH 7.5, 5- mM EDTA, 5-mM EGTA, 10-mM DTT, 10-mM Na_3VO_4, 10-mM NaF, 50-mM β-glycerophosphate, 1-mM PMSF, 5-μg/mL leupeptin, 5-μg/mL antipain, 5-μg/mL aprotinin, 5% [v/v] glycerol) and separated by SDS–PAGE containing 2-mg/mL histone as a substrate.

DAP-seq and data analysis

The procedure for DAP-seq and data analysis were carried out as described (Bartlett et al., 2017; Cao et al., 2020; Dou et al., 2021). Tomato (MT) genomic DNA library was prepared using NEBNext DNA Library Prep Master Mix Set Kit for Illumina (NEB, Ipswich, MA, USA). The coding sequence of *SlVOZ1* was cloned in-frame with the *HaloTag* sequence (Promega, Madison, WI, USA); the resulting recombinant SlVOZ1 fusion protein was produced in *E. coli* and purified with HaloTag Beads (Promega). The SlVOZ1-HaloTag bead mixture was incubated with the tomato genomic DNA library under slow rotation at 4°C for ∼2 h, followed by five washes with phosphate-buffered saline buffer. The DNA was eluted from the beads in 25 μL of elution buffer. A negative control was prepared by omitting SlVOZ1-HaloTag protein from the bead mixture. SlVOZ1 target genes were defined as the peaks located within the transcribed regions of genes, introns, 3-kb upstream or downstream of the translation start site (ATG) or termination site (Stop codon). DAP-seq reads were aligned to the reference tomato genome (iTAG3.2). SlVOZ1 binding motifs were identified by MEME-ChIP (Machanick and Bailey, 2011).

RNA extraction and RT–qPCR

Total RNA was isolated using RNAiso Reagent (TaKaRa). RNA quality and concentration were assessed on a NanoDrop 1000 Spectrophotometer (ThermoFisher Scientific, Waltham, MA, USA). First-strand cDNA was synthesized using PrimeScript RT Reagent Kit (TaKaRa) following the manufacturer's instructions from 2 μg of total RNA. For RT–qPCR, reactions were conducted on a QuantStudio 5 instrument (Applied Biosystems, Waltham, MA, USA) with Hieff qPCR SYBR Green Master Mix Kit (YEASEN, Shanghai, China). Primer sequences are provided in Supplemental Table S1. Tomato *Actin 7* was used as a reference control in all gene expression analyses.

ChIP-qPCR

ChIP experiments were performed as described (Saleh et al., 2008; Zhu et al., 2020) with minor modifications. About 1 g of leaves was collected from 6-week-old tomato plants for crosslinking with 1% (w/v) formaldehyde. Chromatin complexes were precipitated with anti-SlVOZ1 antibody and salmon sperm DNA/Protein A agarose (Millipore, Burlington, MA, USA) at 4°C for at least 6 h. The precipitated DNA was purified with DNA Clean & Concentrator (ZYMO RESEARCH Irvine, CA, USA). ChIP-qPCR was performed two independent times with similar results.

Accession numbers

Sequence data from this article can be found in the Tomato Genome Protein Sequences (ITAG release 4.0) database under the following accession numbers: *SlOST1* (Solyc01g108280), *SlVOZ1* (Solyc02g077450), *SlVOZ2* (Solyc10g008880), and *SFT* (Solyc03g063100). The DAP-seq data described in this article have been deposited to NCBI under accession number PRJNA734096 (https://www.ncbi.nlm.nih.gov/bioproject/?term=PRJNA734096).

Supplemental data

The following materials are available in the online version of this article.

Supplemental Figure S1. Subcellular localization of SlOST1 and tissue expression of *SlOST1*.

Supplemental Figure S2. Sequence alignment of SlOST1 target sites in CRISPR lines.

Supplemental Figure S3. Tomato OST1 regulates drought tolerance.

Supplemental Figure S4. Protein sequence alignment of tomato and Arabidopsis VOZ1.

Supplemental Figure S5. *SlVOZ1* expression patterns in tomato tissues.

Supplemental Figure S6. Specificity test of the anti-SlVOZ1 antibody.

Supplemental Figure S7. ABA treatment activates SlOST1 in tomato in in-gel kinase assays.

Supplemental Figure S8. SlVOZ1 translocates from the cytoplasm to the nucleus in *N. benthamiana* leaves.

Supplemental Figure S9. Seed germination phenotype of WT, *slost1* and *slvoz1* mutants in response to ABA treatment.

Supplemental Figure S10. Flowering time of WT, *slost1*, *slvoz1* mutants under normal and drought conditions.

Supplemental Figure S11. *SFT* expression levels in WT, *slost1* and *slvoz1* mutants.

Supplemental Figure S12. Flowering phenotype of the *slost1 slvoz1* double mutant under normal and drought conditions.

Supplemental Table S1. Primer sequences used in this study.

Supplemental Data Set 1. DAP-seq results for SlVOZ1, first replicate.

Supplemental Data Set 2. DAP-seq results for SlVOZ1, second replicate.

Supplemental Data Set 3. Summary of statistical analyses.

Supplemental File S1. Multiple sequence alignment used for the phylogenetic tree shown in Figure 1A.

Supplemental File S2. Newick format of the alignment shown in Figure 1A.

Acknowledgments

We thank Prof. Chun-Peng Song for his suggestions and we acknowledge Dr. Huihui Su, Dr. Zhixin Jiao, Dongling Zhang, and Dr. Huangai Bi for their contributions to the DAP-seq and phenotypic analyses.

Funding

This work was supported by the National Natural Science Foundation of China (NSFC) 32070307, 32150410345 and Henan Science and Technology Development Plan Project 212300410023. This work was also partly supported by the open funds of the State Key Laboratory of Plant Physiology and Biochemistry (SKLPPBKF2107).

Conflict of interest statement. The authors declare that they have no conflict of interest.

References

Ali A, Pardo JM, Yun DJ (2020) Desensitization of ABA-signaling: the swing from activation to degradation. Front Plant Sci **11**: 379

Assmann SM (2003) Open Stomata1 opens the door to ABA signaling in Arabidopsis guard cells. Trends Plant Sci **8**: 151–153

Bao F, Huang X, Zhu C, Zhang X, Li X, Yang S (2014) Arabidopsis HSP90 protein modulates RPP4-mediated temperature-dependent cell death and defense responses. New Phytol **202:** 1320–1334

Bartlett A, O'Malley RC, Huang SC, Galli M, Nery JR, Gallavotti A, Ecker JR (2017) Mapping genome-wide transcription-factor binding sites using DAP-seq. Nat Protoc **12**: 1659–1672

Cao Y, Zeng H, Ku L, Ren Z, Han Y, Su H, Dou D, Liu H, Dong Y, Zhu F, et al. (2020) ZmIBH1-1 regulates plant architecture in maize. J Exp Bot **71:** 2943–2955

Celesnik H, Ali GS, Robison FM, Reddy ASN (2013) *Arabidopsis thaliana* VOZ (vascular plant one-zinc finger) transcription factors are required for proper regulation of flowering time. Biol Open **2**: 424–431

Chen K, Li GJ, Bressan RA, Song CP, Zhu JK, Zhao Y (2020a) Abscisic acid dynamics, signaling, and functions in plants. J Integr Plant Biol **62:** 25–54

Chen Q, Bai L, Wang W, Shi H, Ramón Botella J, Zhan Q, Liu K, Yang HQ, Song CP (2020b) COP1 promotes ABA-induced stomatal closure by modulating the abundance of ABI/HAB and AHG3 phosphatases. New Phytol **229**: 2035–2049

Chong L, Guo P, Zhu Y (2020) Mediator complex: a pivotal regulator of ABA signaling pathway and abiotic stress response in plants. Int J Mol Sci **21:** 7755

Coello P, Hey SJ, Halford NG (2011) The sucrose non-fermenting-1-related (SnRK) family of protein kinases: potential for manipulation to improve stress tolerance and increase yield. J Exp Bot **62**: 883–893

Cui L, Zheng F, Wang J, Zhang C, Xiao F, Ye J, Li C, Ye Z, Zhang J (2020) miR156a-targeted SBP-Box transcription factor SlSPL13 regulates inflorescence morphogenesis by directly activating SFT in tomato. Plant Biotechnol J **18**: 1670–1682

Dou DD, Han SB, Cao LR, Ku LX, Liu HF, Su HH, Ren ZZ, Zhang DL, Zeng HX, Dong YH, et al. (2021) CLA4 regulates leaf angle through multiple hormone signaling pathways in maize. J Exp Bot **72**: 1782–1794

Du H, Huang F, Wu N, Li X, Hu H, Xiong L (2018) Integrative regulation of drought escape through ABA-dependent and -independent pathways in rice. Mol Plant **11:** 584–597

Franks SJ (2011) Plasticity and evolution in drought avoidance and escape in the annual plant Brassica rapa. New Phytol **190:** 249–257

Franks SJ, Sim S, Weis AE (2007) Rapid evolution of flowering time by an annual plant in response to a climate fluctuation. Proc Natl Acad Sci USA **104:** 1278–1282

Fujii H, Chinnusamy V, Rodrigues A, Rubio S, Antoni R, Park SY, Cutler SR, Sheen J, Rodriguez PL, Zhu JK (2009) In vitro reconstitution of an abscisic acid signalling pathway. Nature **462**: 660–664

Fujii H, Verslues PE, Zhu JK (2007) Identification of two protein kinases required for abscisic acid regulation of seed germination, root growth, and gene expression in Arabidopsis. Plant Cell **19**: 485–494

Fujii H, Zhu JK (2009) Arabidopsis mutant deficient in 3 abscisic acid-activated protein kinases reveals critical roles in growth, reproduction, and stress. Proc Natl Acad Sci USA **106**: 8380–8385

Fujii H, Zhu JK (2012) Osmotic stress signaling via protein kinases. Cell Mol Life Sci **69:** 3165–3173

Fujita Y, Nakashima K, Yoshida T, Katagiri T, Kidokoro S, Kanamori N, Umezawa T, Fujita M, Maruyama K, Ishiyama K, et al. (2009) Three SnRK2 protein kinases are the main positive regulators of abscisic acid signaling in response to water stress in Arabidopsis. Plant Cell Physiol **50:** 2123–2132

Fujita Y, Yoshida T, Yamaguchi-Shinozaki K (2013) Pivotal role of the AREB/ABF-SnRK2 pathway in ABRE-mediated transcription in response to osmotic stress in plants. Physiol Plant **147**: 15–27

Geiger D, Scherzer S, Mumm P, Stange A, Marten I, Bauer H, Ache P, Matschi S, Liese A, Al-Rasheid KAS, et al. (2009) Activity of guard cell anion channel SLAC1 is controlled by drought-stress signaling kinase-phosphatase pair. Proc Natl Acad Sci USA **106**: 21425–21430

Guo P, Chong L, Wu F, Hsu C, Li C, Zhu J, Zhu Y (2021) Mediator tail module subunits MED16 and MED25 differentially regulate abscisic acid signaling in Arabidopsis. J Integr Plant Biol **63:** 802–815

Helliwell CA, Wood CC, Robertson M, James Peacock W, Dennis ES (2006) The Arabidopsis FLC protein interacts directly in vivo with SOC1 and FT chromatin and is part of a high-molecular-weight protein complex. Plant J **46:** 183–192

Hou YJ, Zhu Y, Wang P, Zhao Y, Xie S, Batelli G, Wang B, Duan CG, Wang X, Xing L, et al. (2016) Type one protein phosphatase 1 and its regulatory protein inhibitor 2 negatively regulate ABA signaling. PLoS Genet **12:** e1005835

Hsu CC, Zhu Y, Arrington JV, Paez JS, Wang P, Zhu P, Chen IH, Zhu JK, Tao WA (2018) Universal plant phosphoproteomics workflow and its application to tomato signaling in response to cold stress. Mol Cell Proteomics **17**: 2068–2080

Joshi-Saha A, Valon C, Leung J (2011) Abscisic acid signal off the STARTing block. Mol Plant **4:** 562–580

Kong L, Cheng J, Zhu Y, Ding Y, Meng J, Chen Z, Xie Q, Guo Y, Li J, Yang S, et al. (2015) Degradation of the ABA co-receptor ABI1 by PUB12/13 U-box E3 ligases. Nat Commun **6:** 8630

Krieger U, Lippman ZB, Zamir D (2010) The flowering gene SINGLE FLOWER TRUSS drives heterosis for yield in tomato. Nat Genet **42:** 459–463

Kulik A, Wawer I, Krzywińska E, Bucholc M, Dobrowolska G (2011) SnRK2 protein Kinases - Key regulators of plant response to abiotic stresses. OMICS **15:** 859–872

Kumar S, Stecher G, Tamura K (2016) MEGA7: molecular evolutionary genetics analysis version 7.0 for bigger datasets. Mol Biol Evol **33:** 1870–1874

Kumar S, Choudhary P, Gupta M, Nath U (2018) VASCULAR PLANT ONE-ZINC FINGER1 (VOZ1) and VOZ2 interact with constans and promote photoperiodic flowering transition. Plant Physiol **176:** 2917–2930

Lang Z, Wang Y, Tang K, Tang D, Datsenka T, Cheng J, Zhang Y, Handa AK, Zhu JK (2017) Critical roles of DNA demethylation in the activation of ripening-induced genes and inhibition of ripening-repressed genes in tomato fruit. Proc Natl Acad Sci USA **114:** E4511–E4519

Lee SC, Lan W, Buchanan BB, Luan S (2009) A protein kinase-phosphatase pair interacts with an ion channel to regulate ABA signaling in plant guard cells. Proc Natl Acad Sci USA **106**: 21419–21424

Lifschitz E, Eshed Y (2006) Universal florigenic signals triggered by FT homologues regulate growth and flowering cycles in perennial day-neutral tomato. J Exp Bot **57:** 3405–3414

Lifschitz E, Eviatar T, Rozman A, Shalit A, Goldshmidt A, Amsellem Z, Alvarez JP, Eshed Y (2006) The tomato FT ortholog triggers systemic signals that regulate growth and flowering and substitute for diverse environmental stimuli. Proc Natl Acad Sci USA **103:** 6398–6403

Machanick P, Bailey TL (2011) MEME-ChIP: motif analysis of large DNA datasets. Bioinformatics **27:** 1696–1697

Mao G, Meng X, Liu Y, Zheng Z, Chen Z, Zhang S (2011) Phosphorylation of a WRKY transcription factor by two pathogen-responsive MAPKs drives phytoalexin biosynthesis in Arabidopsis. Plant Cell **23**: 1639–1653

Mao Y, Zhang H, Xu N, Zhang B, Gou F, Zhu JK (2013) Application of the CRISPR–Cas system for efficient genome engineering in plants. Mol Plant **6:** 2008–2011

Martignago D, Siemiatkowska B, Lombardi A, Conti L (2020) Abscisic acid and flowering regulation: many targets, different places. Int J Mol Sci **21:** 9700

Mimida N, Kidou SI, Iwanami H, Moriya S, Abe K, Voogd C, Varkonyi-Gasic E, Kotoda N (2011) Apple FLOWERING LOCUS T proteins interact with transcription factors implicated in cell growth and organ development. Tree Physiol **31**: 555–566

Mitsuda N, Hisabori T, Takeyasu K, Sato MH (2004) VOZ; isolation and characterization of novel vascular plant transcription factors with a one-zinc finger from *Arabidopsis thaliana*. Plant Cell Physiol **45:** 845–854

Molinero-Rosales N, Latorre A, Jamilena M, Lozano R (2004) SINGLE FLOWER TRUSS regulates the transition and maintenance of flowering in tomato. Planta **218**: 427–434

Mustilli AC, Merlot S, Vavasseur A, Fenzi F, Giraudat J (2002) Arabidopsis OST1 protein kinase mediates the regulation of stomatal aperture by abscisic acid and acts upstream of reactive oxygen species production. Plant Cell **14**: 3089–3099

Nakai Y, Nakahira Y, Sumida H, Takebayashi K, Nagasawa Y, Yamasaki K, Akiyama M, Ohme-Takagi M, Fujiwara S, Shiina T, et al. (2013a) Vascular plant one-zinc-finger protein 1/2 transcription factors regulate abiotic and biotic stress responses in Arabidopsis. Plant J **73:** 761–775

Nakai Y, Fujiwara S, Kubo Y, Sato MH (2013b) Overexpression of VOZ2 confers biotic stress tolerance but decreases abiotic stress resistance in Arabidopsis. Plant Signal Behav **8**: 2–5

Nakashima K, Fujita Y, Kanamori N, Katagiri T, Umezawa T, Kidokoro S, Maruyama K, Yoshida T, Ishiyama K, Kobayashi M, et al. (2009) Three Arabidopsis SnRK2 protein kinases, SRK2D/SnRK2.2, SRK2E/SnRK2.6/OST1 and SRK2I/SnRK2.3, involved in ABA signaling are essential for the control of seed development and dormancy. Plant Cell Physiol **50:** 1345–1363

Nakashima K, Yamaguchi-Shinozaki K (2013) ABA signaling in stress-response and seed development. Plant Cell Rep **32:** 959–970

Navarro C, Abelenda JA, Cruz-Oro E, Cuellar CA, Tamaki S, Silva J, Shimamoto K, Prat S (2011) Control of flowering and storage organ formation in potato by FLOWERING LOCUS T. Nature **478**: 119–122

Prasad K, Xing D, Reddy A (2018) Vascular plant one-zinc-finger (VOZ) transcription factors are positive regulators of salt tolerance in Arabidopsis. Int J Mol Sci **19**: 3731

Rothan C, Diouf I, Causse M (2019) Trait discovery and editing in tomato. Plant J **97**: 73–90

Reichardt S, Piepho HP, Stintzi A, Schaller A (2020) Peptide signaling for drought-induced tomato flower drop. Science **367**: 1482–1485

Riboni M, Galbiati M, Tonelli C, Conti L (2013) GIGANTEA enables drought escape response via abscisic acid-dependent activation of the florigens and SUPPRESSOR OF OVEREXPRESSION OF CONSTANS. Plant Physiol **162:** 1706–1719

Saleh A, Alvarez-Venegas R, Avramova Z (2008) An efficient chromatin immunoprecipitation (ChIP) protocol for studying histone modifications in Arabidopsis plants. Nat Protoc **3:** 1018–1025

Sato A, Sato Y, Fukao Y, Fujiwara M, Umezawa T, Shinozaki K, Hibi T, Taniguchi M, Miyake H, Goto DB, et al. (2009) Threonine at position 306 of the KAT1 potassium channel is essential for channel activity and is a target site for ABA-activated SnRK2/OST1/SnRK2.6 protein kinase. Biochem J **424**: 439–448

Schwarzenbacher RE, Wardell G, Stassen J, Guest E, Zhang P, Luna E, Ton J (2020) The IBI1 receptor of β-aminobutyric acid interacts with VOZ transcription factors to regulate abscisic acid signaling and callose-associated defense. Mol Plant **13**: 1455–1469

Selote D, Matthiadis A, Gillikin JW, Sato MH, Long TA (2018) The E3 ligase BRUTUS facilitates degradation of VOZ1/2 transcription factors. Plant Cell Environ **41**: 2463–2474

Shavrukov Y, Kurishbayev A, Jatayev S, Shvidchenko V, Zotova L, Koekemoer F, de Groot S, Soole K, Langridge P (2017) Early flowering as a drought escape mechanism in plants: how can it aid wheat production? Front Plant Sci **8**: 1950

Sherrard ME, Maherali H (2006) The adaptive significance of drought escape in Avena barbata, an annual grass. Evolution **60:** 2478–2489

Silva GFF, Silva EM, Correa JPO, Vicente MH, Jiang N, Notini MM, Junior AC, De Jesus FA, Castilho P, Carrera E, et al. (2019) Tomato floral induction and flower development are orchestrated by the interplay between gibberellin and two unrelated microRNA-controlled modules. New Phytol **221:** 1328–1344

Song YH, Ito S, Imaizumi T (2013) Flowering time regulation: photoperiod- and temperature-sensing in leaves. Trends Plant Sci **18**: 575–583

Soyk S, Muller NA, Park SJ, Schmalenbach I, Jiang K, Hayama R, Zhang L, Van Eck J, Jimenez-Gomez JM, Lippman ZB (2017) Variation in the flowering gene SELF PRUNING 5G promotes day-neutrality and early yield in tomato. Nat Genet **49:** 162–168

Takeno K (2016) Stress-induced flowering: the third category of flowering response. J Exp Bot **67:** 4925–4934

Tsuji H, Taoka K, Shimamoto K (2011) Regulation of flowering in rice: two florigen genes, a complex gene network, and natural variation. Curr Opin Plant Biol **14**: 45–52

Wang P, Xue L, Batelli G, Lee S, Hou YJ, Van Oosten MJ, Zhang H, Tao WA, Zhu JK (2013) Quantitative phosphoproteomics identifies SnRK2 protein kinase substrates and reveals the effectors of abscisic acid action. Proc Natl Acad Sci USA **110:** 11205–11210

Weng L, Bai X, Zhao F, Li R, Xiao H (2016) Manipulation of flowering time and branching by overexpression of the tomato transcription factor SlZFP2. Plant Biotechnol J **14:** 2310–2321

Yasui Y, Mukougawa K, Uemoto M, Yokofuji A, Suzuri R, Nishitani A, Kohchia T (2012) The phytochrome-interacting VASCULAR PLANT ONE-ZINC FINGER1 and VOZ2 redundantly regulate flowering in Arabidopsis. Plant Cell **24:** 3248–3263

Yoshida R, Hobo T, Ichimura K, Mizoguchi T, Takahashi F, Aronso J, Ecker JR, Shinozaki K (2002) ABA-activated SnRK2 protein kinase is required for dehydration stress signaling in Arabidopsis. Plant Cell Physiol **43:** 1473–1483

Yu H, Xu Y, Tan EL, Kumar PP (2002) AGAMOUS-LIKE 24, a dosage-dependent mediator of the flowering signals. Proc Natl Acad Sci USA **99**: 16336–16341

Zhu JK (2016) Abiotic stress signaling and responses in plants. Cell **167**: 313–324

Zhu Y, Schluttenhoffer CM, Wang P, Fu F, Thimmapuram J, Zhu JK, Lee SY, Yun DJ, Mengiste T (2014) CYCLIN-DEPENDENT KINASE8 differentially regulates plant immunity to fungal pathogens through kinase-dependent and -independent functions in Arabidopsis. Plant Cell **26**: 4149–4170

Zhu Y, Huang P, Guo P, Chong L, Yu G, Sun X, Hu T, Li Y, Hsu CC, Tang K, et al. (2020) CDK8 is associated with RAP2.6 and SnRK2.6 and positively modulates abscisic acid signaling and drought response in Arabidopsis. New Phytol **228**: 1573–1590